The role of the metastasis promoting protein S100A4 during EMT in mammary gland epithelial cells

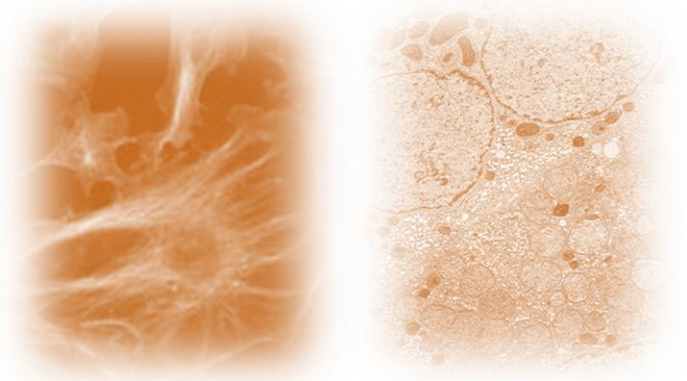

Vibeke Wethe Rognlien

2013

OSLO AND AKERSHUS
UNIVERSITY COLLEGE
OF APPLIED SCIENCES

The role of the metastasis promoting protein S100A4 during EMT in mammary gland epithelial cells

By

Vibeke Wethe Rognlien

Master i Biomedisin
Faculty of Health Sciences
Oslo and Akershus University college of Applied Sciences

Master thesis, 60 study points.

Written at the Department of Tumor Biology,
Institute of Cancer Research
Oslo University Hospital
The Norwegian Radium Hospital

May 21th, 2013

Acknowledgements

The process of working with this thesis was been a great personal experience, and I would especially like to express a lot of gratitude to my supervisor Dr. Kristin Andersen for helping me with both laboratory techniques as well as helping me understand the results of my experiments. Thank you for encouragement during time of frustration.

I would also like to thank Professor Gunhild Mælandsmo for welcoming me into her group and for showing interest in my project. Your inputs have been very helpful.
The members of Gunhild's S100-group have also been of invaluable help. Thank you all for professional feedback, and especially thanks to Dr. Gisle Berge, MSc Solveig Pettersen, technician Tove Øygård, Dr. Ellen Tenstad and Dr. Birgit Engesæter, as well as Dr. Else Munthe of senior researcher Dr. Ola Myklebost group, for helping me with laboratory technics.

I am very grateful to have had the opportunity to work with my thesis at the Department of Tumor Biology. It has been a great educational environment, and I would like to thank all the other master students I have meet during my time here for valuable input and help, as well as sharing of frustration.

Finally, I would like to thank my family and friends for all their love and support, and especially Jon Tunby Kritiansen. I could honestly never have done this without your comfort and encouragement.

Oslo 2013

Vibeke Wethe Rognlien

Abstract

Breast cancer is one of the greatest contributors to mortality among the different cancer types in the female population of the western world each year. An increasing degree of evidence state that the S100A4 protein, which has been identified in several tumors of different origins and has proven to be associated with a poor patient prognosis, might have an important role in a process which induces carcinoma cells of the breast to gain a more motile and invasive phenotype. This process, which enables metastasis of carcinoma cells, is termed epithelial-to-mesenchymal transition (EMT).

In the current study, immortalized human mammary epithelial cells were used to investigate non-cancerous epithelial cells ability to undergo EMT when the expression of S100A4 had been knocked down by lentiviral transduction. The knock-down cells were subsequently stimulated with TGF-β1 for eight days to induce EMT.

In order to evaluate whether the epithelial cells had undergone EMT, established markers identifying mesenchymal status of the cells were tested, including morphology observed by phase contrast microscopy, mRNA expression of several biological markers associated with EMT, as well as immunofluorescence staining of E-cadherin observed by microscopy to monitor any change in the cells distribution pattern. The observed results indicate that the epithelial cells of the HMLE cell line, regardless of expressing S100A4 or not, were able to gain mesenchymal characteristics as a result of TGF-β1 stimulation, indicating an ability to undergo EMT even though the cells are not expressing S100A4.

Sammendrag

Blant kvinner i den vestlige verden er dødesfall som følge av brystkreft en av hovedårsakene til kreftrelatert dødelighet hvert år. S100A4 proteinet har blitt identifisert i flere krefttyper av ulik opprinnelse, og tilstedeværelse av proteinet assosieres ofte med dårlig sykdomsprognose. Det antas at S100A4 spiller en viktig rolle i en biologisk prosess hvor karsinomceller induseres til å uttrykke biologiske markører assosiert med mesenkymale celler. Denne prosessen, som gir kreftcellene økt metastatisk potensiale, kalles epitelial-til-mesenkymal transisjon (EMT).

HMLE cellelinjen bestående av immortaliserte epitelceller fra bryst ble benyttet for å undersøke normale epitelceller fra bryst (ikke kreftceller) sin evne til å gjennomgå EMT når utrykket av S100A4 var slått av ved hjelp av lentivirus transduksjon. Cellene hvor S100A4 var blitt slått av ble senere stimulert med TGF-β1 i åtte dager for å indusere EMT.

For å kunne avgjøre om epitelcellene hadde gjennomgått EMT, ble utrykket av etablerte biologiske markører assosiert med mesenkymal status evaluert. Mesenkymal status ble evaluert ut i fra morfologi, grad av mRNA uttrykt av ulike biologiske markørene assosiert med EMT, samt immunofluorescens farging av celler dyrket på dekkglass for å påvise cellulær distribusjon av E-caderin. Resultatene av disse testene indikerte at epitelcellene fra HMLE cellelinjen kunne gjennomgå EMT som et resultat av TGF-β1 stimulering, uavhengig av om de uttrykker S100A4 eller ikke.

Abbreviations

AII	Annexin II
BCA	Bicinchoninic acid
BSA	Bovine Serum Albumin
CCN3	Nephroblastoma Overexpressed Gene (NOV)
c-DNA	complementary DNA
C_q	Quantification cycle
DAPI	4',6-diamidino-2-phenylindole
DCIS	Ductal Carcinoma In Situ
DMEM/F12	Dulbecco's Modified Eagle Medium: Nutrient Mixture F12
DMSO	Dimethyl sulfoxide
DNA	Deoxyribonucleic acid
ECM	Extracellular matrix
EGF	Epithelial Growth Factor
EMT	Epithelial-to-mesenchymal transition
EMT-ATFs	EMT-Activating Transcription Factors
EpCAM	Epithelial cell Adhesion Molecule
FACS	Fluorescence-Activated Cell Sorting
FCS	Fetal Calf Serums
FGF	Fibroblast Growth Factor
FRET	Fluorescence Resonance Energy Transfer
FSC	Forward Scatter
Hexa	Hexadimethrine bromide
HGF	Hepatocyte Growth Factor
HMEC	Human Mammary Epithelial Cell
HMLE	Immortalized Human Mammary Epithelial Cells
HRP	Horseradish peroxidase
IDC	Invasive Ductal Carcinoma
IGF	Insulin-like Growth Factor
ILC	Invasive Lobular Carcinoma
IMS	Immunomagnetic separation
LCIS	Lobular Carcinoma In Situ
LDS	Lithium Dodecyl Sulfate
MAPK	Mitogen-Activated Protein Kinases
MEGM	Mammary Epithelial Cell Growth Medium
MET	Mesenchymal-to-epithelial transition

miR200/205	MicroRNA 200/205
MMP	Matrix Metalloproteinase
MOI	Multiplicity of Infection
mRNA	Messenger RNA
NF-κB	Nuclear Factor-κB
NH_4Cl	Ammonium Chloride
NMMHC	Nonmuscle Myosin Heavy Chain
P37/P53	Protein 37/53
PBS	Phosphate Buffered saline
PDGF	Platlet-Derived Growth Factor
PFA	Paraformaldehyde
PMT	Photomultiplier tube
Puro	Puromycin
RAGE	Receptor for Advanced Glycation End products
RIPA	Radio Immuno Precipitation Assay buffer
RISC	RNA Induced Silencing Complex
RNase	Ribonuclease
RNA	Ribonucleic acid
RNAi	RNA interference
rS100A4	Recombinant S100A4
R-Smad	Receptor activated Smad
RT-qPCR	Reverse Transcription Quantitative Polymerase Chain Reaction
SDS	Sodium Dodecyl Sulfate
Shctr	HMLE cells transtuced with control vector
shA4	HMLE cells transduced with anti-S100A4 virus
Shh	Sonic Hedgehog
shRNA	Short hairpin RNA
SNAI1	Snail
SNAI2	Slug
SSC	Side Scatter
Taq	*Thermus aquaticus*
TDLU	Terminal Duct Lobular Unit
TEB	Terminal End Bud
TGF-β	Transforming Growth Factor-β
tPA	Tissue Plasminogen Activator
TRITC	Tetramethylrhodamine-5-(and-6)-isothiocyanate
ZEB	Zinc finger E-box Binding homeobox

Contents

Introduction

1.1 Aim of the study

The aim of the study was to elucidate the role of S100A4 during EMT in mammary gland epithelial cells. More specifically, to determine whether the expression of S100A4 was necessary for induction of EMT in mammary gland epithelial cells.

EMT is a regulatory process where epithelial cells are induced to express mesenchymal characteristics, and acquire e.g. cell motility. EMT is observed in both normal physiological development of e.g. the ductal structure of the breast and during embryonic development, as well as in invasive cancers with epithelial origin. The process of EMT is associated with increased metastatic potential and invasiveness of e.g. carcinoma cells of the breast [1].

One of S100A4's many features is its ability to induce increased capability to migrate. The biological functions include regulation of angiogenesis, cell survival, motility, and invasion. S100A4 has been found expressed in mesenchymal cells that have undergone epithelial-to-mesenchymal transition (EMT) in, amongst other, human mammary epithelial cells [2, 3]. Furthermore, several studies have established S100A4 expression in biopsies from breast cancer patients to be associated with poorer prognosis [4, 5]. It was therefore of great interest to investigate the role of S100A4 during EMT. Knowledge on how cancer cells acquire cell motility might reveal new possibilities for targeted inhibition of their metastatic potential.

1.2 Mammary gland development

The development of the mammary gland is conducted mainly through branching morphogenesis, primarily during adolescence. This differs from other branched tissues where the branching morphogenesis mainly occurs during fetal development [6]. The process of mammary branching can be divided into three phases with different regulating aspects; embryonic, adolescence and pregnancy. The development during the embryonic phase is hormone independent. The formation of bilateral mammary ducts (milk lines) in a tree-like structure starts and is present in a small portion of the mammary fat pad at birth [6, 7]. Undifferentiated mesenchymal cells start to involute from the epidermis to form primary buds. Secondary buds start to form from the primary buds, developing a branched structure of lactiferous ducts (Figure 1.1) [8]. After birth, the commenced structure of the mammary gland undergoes involution and the remaining ducts acquires a quiescent state until the onset of puberty [6].

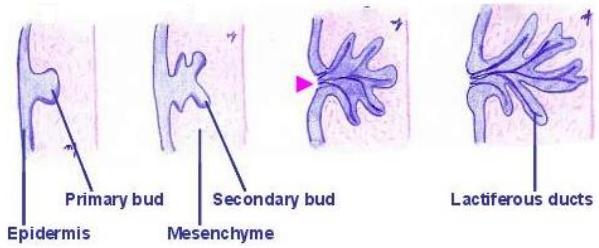

Figure 1.1 Development of lactiferous ducts from the epidermis during the embryonic phase. The image is adapted from *Joseph, N., 2012* [8].

The branching during adolescence is dependent on several hormones secreted from the ovaries and the pituitary gland, such as estrogen, progesterone, growth hormones and prolactin [7]. Terminal end buds (TEBs) starts to form on the end of the ducts resulting in further penetration of the mesenchymal fat pad as the ducts elongate. Branching of the TEBs creates new ducts and secondary side-branches starts sprouting to fill the entire fat pad with a comprehensive system of branched ducts. The branching ceases when it reaches the outer limits of the mesenchymal fat pad [6, 9].

Further development of the human breast begins when the female becomes pregnant. Estrogen and progesterone levels are elevated to ensure that the mammary glands becomes fully developed. A human breast consists of between 12 to 20 milk glands termed lobuli, which again are divided in even smaller glands containing both alveoli and an intralobular terminal duct. This comprises the functional unit of the breast, termed terminal duct lobular unit (TDLU), and is responsible for milk production during lactation. The milk is then guided through the ducts to the nipple [7, 8].

1.3 Breast cancer

In 2008, breast cancer related deaths were reported to be 458 000 on a worldwide basis [10]. Breast cancer is among the most frequent types, along with lunge, stomach, liver and colon cancer, and it is the most frequent cancer type amongst the female population in the western world, including Norway [11]. The characterization of premalignancy is determined histologically by detection of abnormal proliferation in either the ductal or the lobular cells. In premalignancies the basement membrane is still intact. Once the cells have penetrated the basement membrane, the cancer is characterized as an invasive carcinoma [12].

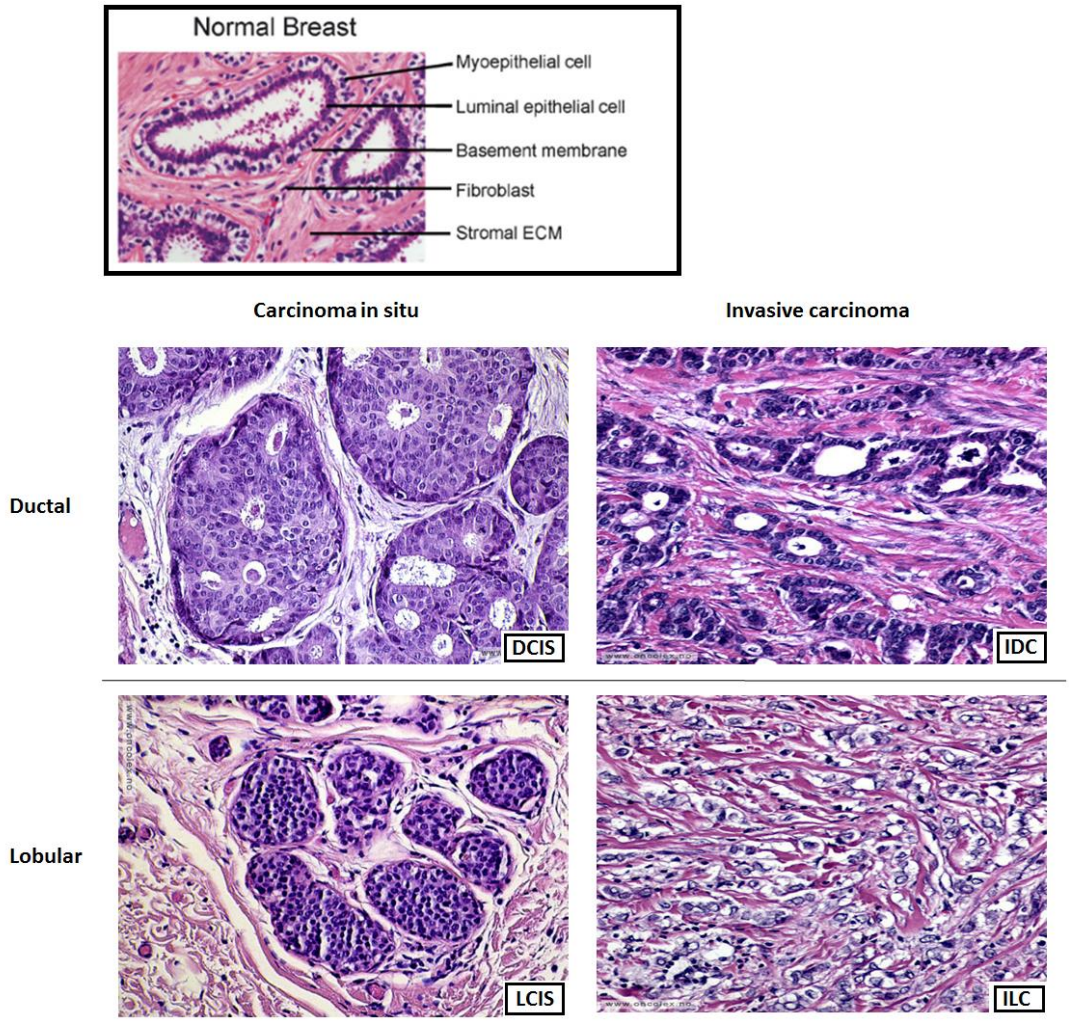

Figure 1.2 All the images show hematoxylin and eosin staining of histological sections of a human breast. The image at the top illustrates normal organization of a human breast (Adapted from [13]). The four subsequent images illustrate different versions of cancer progression. The two vertical images to the left show carcinoma in situ, both ductal (DCIS) and lobular (LCIS), where epithelial cells have started to fill the ducts/lobules. The basement membrane is still intact (in situ). The two vertical images to the right show invasive carcinoma cells, both ductal (IDC) and lobular (ILC). In these cases, the carcinoma cells have penetrated the basement membrane and become invasive (All adapted from [12]).

Carcinomas originates from epithelial cells. There are several subtypes of breast carcinomas, and about 90 % are invasive ductal carcinomas (IDC). Only 5-10 % of the tumors are invasive lobular carcinomas (ILC), originating from the intralobular epithelium [8, 14]. Before the tumors turns invasive, they are referred to as ductal carcinoma in situ (DCIS) and lobular carcinoma in situ (LCIS). Examples of histopathology of the main types of breast cancer is shown in Figure 1.2. Once invasive, they undergo a very strong desmoplastic reaction. A desmoplastic reaction is "*a connective tissue stromal reaction to the tumor*", which makes the tumor very firm. Because of this, these types of tumors are also referred to as *scirrhous carcinomas*. A typical symptom of breast cancer is retraction of the nipple, and is caused by the underlying tumor pulling on its adjacent tissue [14].

45 % of all breast carcinomas are found in the upper lateral quadrant, while 25 % are found just underneath the areola (Figure 1.3). The size of the tumor may vary, but most tumors range from 1 cm to several centimeters in diameter. By self-examination, the smallest tumor one is able to detect is 2-2.5 cm in diameter. In contrary, by mammography one is able to detect tumors down to the size of 1 cm in diameter [14].

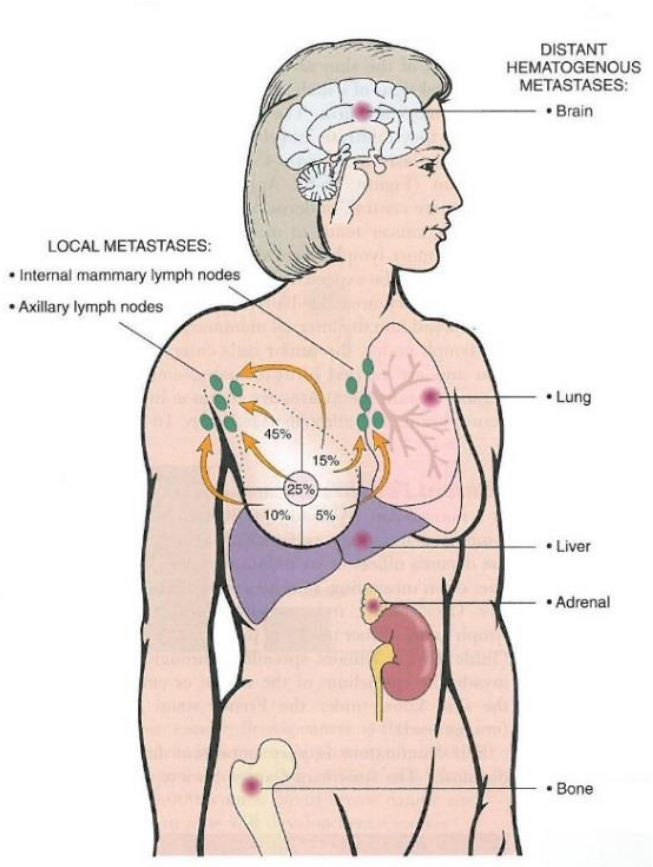

Figure 1.3 Distribution of cancerous disease originating in the epithelial cells of the breast (carcinoma), and their pathway of both lymphatic and hematogenous metastases. The image is adapted from Ivan Damjanov's *Pathology of the Health Professions* [14].

1.4 Metastasis

Metastasis is one of the six hallmarks of cancer described by *Hanahan and Weinberg, 2011* [15]. When a cancer cell acquires invasive properties and subsequently invade the basement membrane, the cancer cells are able to metastasize to new locations through adjacent blood and/or lymphatic vessels, a process that may have life-threatening consequences [10, 16, 17]. Once the cancer has metastasized to another part of the body, the chances of survival are dramatically reduced, and it is estimated that 90 % of all cancer related deaths are caused by metastasis. Breast cancer cells will most frequently metastasize via the lymphatic system. Most of the cancer cells metastasize through the axillary lymph nodes where the majority of the lymph ducts are drained. Hematogenous metastasis caused by breast cancer is most frequent in lungs, liver, bones, brain and adrenals as illustrated in Figure 1.3 [14].

The process in which invasive cancer cells penetrate the basement membrane and enters a circulatory system, either blood or lymphatic, is referred to as intravasation. The subsequent infiltration of a new location is termed extravasation. In the new location, the cancer cell will form micrometastases, which eventually start to colonize. This process is illustrated in Figure 1.5 [16, 17]. Through animal models, it has been estimated that only about 0.01 % of micrometastases will be able to colonize and give rise to macrometastases [18].

Metastasizing cancer cells from breast tumors differs extensively in their colonizing behavior compared to e.g. cancer cells origination from the lungs where distant macrometastases can be detected just months after diagnosis. In the case of breast tumors, macrometastases may not occur until several years or decades after remission due to metastatic latency [19].

Nguyen et al., 2009, describes genes that determine metastatic behavior as metastasis initiation genes. Processes driven by these kind of genes include increased cell motility, epithelial-to-mesenchymal transition (EMT), extracellular matrix degradation, bone marrow progenitor mobilization, angiogenesis and evasion of the immune system [19].

E-cadherin is a biological marker expressed in epithelial cells, and thus also carcinoma cells. A link between increasing degrees of malignancy with decreasing levels of E-cadherin is a characteristic alteration seen in carcinoma cells. E-cadherin is a calcium dependent adhesion molecule with five extracellular calcium binding domains providing intercellular adhesion. This cell-cell adhesion causes the epithelial cells to gather in a cubical sheet formation. Downregulation of this gene causes dissolution of the intercellular adhesion, leading to the detachment from neighboring cells. Another characteristic alteration seen in carcinoma cells correlated with increasing malignancy is upregulation of N-cadherin, Vimentin and S100A4. N-cadherin is under normal circumstances expressed in

migrating neurons and mesenchymal cells during organogenesis [15, 20, 21]. Vimentin is a type III intermediate filament (IF) protein, and is the major cytoskeletal component of mesenchymal cells [22]. S100A4 is a small calcium binding protein responsible for e.g. transcriptional regulation of E-cadherin [2]. These alterations in the cells expression pattern are characteristic for cells that have undergone EMT [15, 23].

1.5 Epithelial-to-mesenchymal transition

Several studies throughout the last decade indicate that solid tissue carcinoma cells gain an invasive and motile phenotype through a developmental regulatory program termed epithelial-to-mesenchymal transition [24]. EMT describes the process through which epithelial cells changes their morphology and phenotypic expression and gain mesenchymal characteristics (Figure 1.4) [25]. The morphologic alteration causes the epithelial cells to lose their cubical formation and become elongated, pointy, and grow with less cell-cell contact. The epithelial cells undergoing EMT also change their polarity from apical-basal to front-back and gain motility as a result from reconstruction of the actin cytoskeleton [1].

Cells possessing a mesenchymal phenotype is associated with increased capacity to migrate, increased invasiveness, elevated resistance to apoptosis, and an elevated production of extracellular matrix (ECM) components [16]. Cells possessing mesenchymal characteristics are thus able to invade adjacent blood and lymphatic vessels, causing migration to other parts of the body [26].

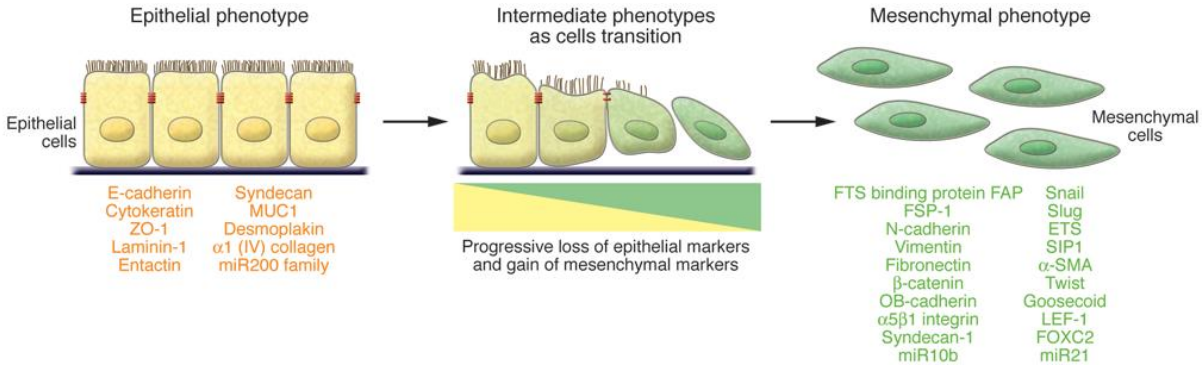

Figure 1.4 Both epithelial and mesenchymal cells illustrated with a listing of cell markers used by researchers to define their cellular state. The transition from epithelial to mesenchymal cells involves progressive loss of epithelial markers and gain of mesenchymal markers. The image is adapted from *Kalluri and Weinberg, 2009* [16].

Some of the processes regulating EMT induction include activation of transcription factors, expression of specific cell surface proteins, reorganization and expression of cytoskeletal proteins, production of

ECM-degrading enzymes, and changes in the expression of specific mircoRNAs [16]. The initial mechanisms inducing EMT is not fully known. A better understanding will enable diagnostic advances facilitating identification of the cancers metastatic potential as well as development of targeted therapy to prevent metastasis [23].

The process of EMT might occur as either transient or stable, and in carcinoma cells, EMT is reversible through mesenchymal-to-epithelial transition (MET), as illustrated in Figure 1.5 [1, 15, 23]. The reestablishment of epithelial cells at the new location poses somewhat of a problem in the research of EMT. MET causes the cells colonizing at a new location to re-express epithelial markers, making them resemble the primary tumor on a histopathological level. It is thus hard to say something about these cells progression through EMT. *Kalluri and Weinberg, 2009*, report the migrating cancer cells no longer receive the signals needed to sustain a mesenchymal character from the stroma of the new localization, and thus undergo MET [16].

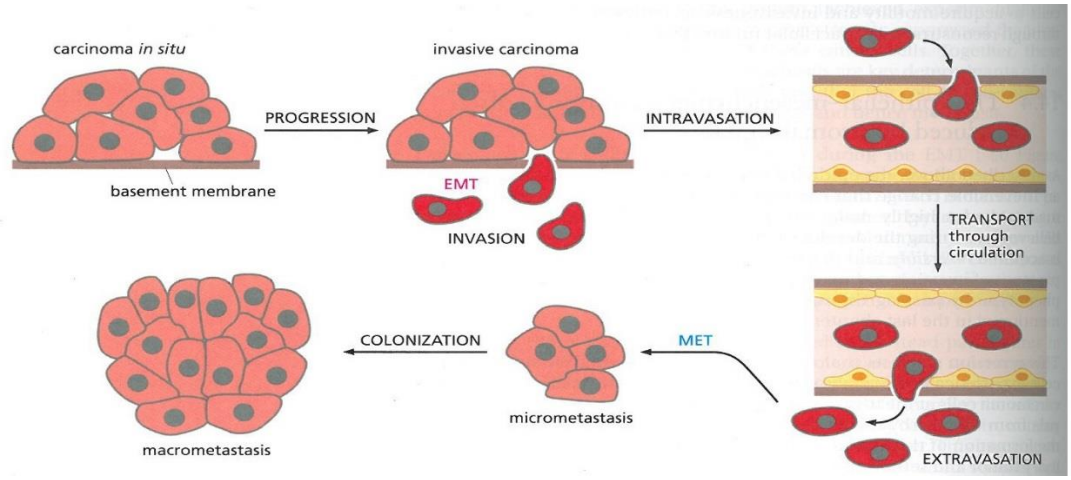

Figure 1.5 The process through which carcinoma cells cease their cubical formation to become cells with mesenchymal characteristics, which in turn invade and metastasize to new parts of the body. This process is reversible through MET. The image is adapted from Robert A. Weinberg's *The Biology of Cancer* [27].

EMT is classified into three subtypes based on the biological process they occur in. Type 1 EMT plays an important role during the embryogenesis and development of the neural crest [1, 16, 23, 26, 28]. Type 2 EMT is induced as a result to inflammation, especially due to wound healing, tissue regeneration, and organ fibrosis. Unlike type 1 EMT where epithelial cells gain mesenchymal characteristics, type 2 EMT induces the transition of epithelial or endothelial cells to fibroblast [1, 16]. Type 3 EMT is associated with the transition of epithelial cancer cells to mesenchymal cells, enabling them to secede from their neighboring cells, invade adjacent tissue, and migrate to new locations [1, 16, 23, 28]. Through numerous studies, a well-established biological marker for both normal physiological EMT as well as for EMT during metastatic progression is S100A4 [2].

1.5.1 EMT initiating factors

During the process of EMT, epithelial cells, primarily on the outer edge of the tumor, receive several signals released from the tumor-associated stroma [27]. These signals, including transforming growth factor-β (TGF-β), epithelial growth factor (EGF), and hepatocyte growth factor (HGF), activate a series of EMT-inducing transcription factors, e.g. Snail (SNAI1), Slug (SNAI2), zinc finger E-box binding homeobox 1 and 2 (ZEB1/2), and Twist [1, 16, 26]. Especially TGF-β is thought to play an important role in conveying these signals and enable induction of EMT [27].

Activated transcription factors will, often in association with each other, choreograph the process of EMT [16]. *Sánchez-Tilló et al., 2012* portrays members of the ZEB, SNAI and Twist families as the three major groups orchestrating EMT, termed EMT-ATFs (EMT-activating transcription factors) [20]. Recent studies report that the EMT-ATFs govern different parts of the EMT process. During initiation of EMT, SNAI1 is found to be the most active, while SNAI2, ZEB1/2 and Twist are thought to sustain the mesenchymal status of the cells [29].

Snail and Slug as well as ZEB1 and ZEB2 are all able to repress expression of E-cadherin in human breast cancer by direct inhibition of the E-cadherin promoter [29, 30]. Snail has also been reported to induce S100A4 expression in cancer cells undergoing EMT [2], and its presence is associated with increased motility and invasiveness [29]. Elevated levels of Twist have been detected in several invasive mammary lobular carcinomas, as well as in invasive ductal carcinoma, but to a much lower extent, and is reported to indirectly repress transcription of E-cadherin [29, 30]. The expression of Twist is induced by e.g. exposure to TGF-β. Expression of Twist and Slug enables resistance to apoptosis, protecting metastasizing cells from physiological stress that otherwise would kill them before they could undergo extravasation and form micrometastases at a new location [30].

Many of these EMT-inducing factors may also alter the ECM, resulting in upregulation of e.g. fibronection, collagen, proteases such as matrix metalloproteinases (MMPs), and other remodeling enzymes [1]. The MMPs may enable detachment of the epithelial cells by cleavage of E-cadherin [24].

One effect TGF-β has in EMT-initiation is activation of the Notch signaling pathway which in turn activates the nuclear factor-κB (NF-κB) pathway, resulting in downregulation of E-cadherin [1]. β-catenin is a structural adaptor protein linking cadherins to the actin cytoskeleton in cell-cell adhesion [31]. The downregulation of E-cadherin will in turn result in release of β-catenin that will move from the cytoplasm to the nucleus, participating in the Wnt-signaling pathway. Wnt-signaling is associated with high levels of Snail in the nucleus. Snail binds to the promoter of E-cadherin, further repressing E-cadherin expression. The loss of E-cadherin will make the cells more sensitive to EMT-inducing

signals [16, 24]. MicroRNA 200 (miR200) and miR205 will inhibit some of the factors repressing E-cadherin expression, with ZEB1/2 as prominent targets. Loss of miR200 is associated with increased levels of vimentin and decreased levels of E-cadherin [1, 16].

1.5.2 TGF-β1

Transforming growth factor beta 1, or TGF-β1, is a member of the transforming growth factor beta family of cytokines. The members of this family are most commonly found to act as local mediators of several biological functions including proliferation, differentiation, extracellular matrix production, apoptosis and migration. TGF-β acts as a tumor suppressor gene restricting cells proliferation of e.g. epithelial cells. In a variety of malignant processes a loss-of-function in the TGF-β protein (or Smad4) has been observed, consequently leading to cancer progression [32, 33].

TGF-β binds to an enzyme-coupled receptor which subsequently causes phosphorylation of Smad2 or Smad3, and the receptor-activated Smad (R-Smad) protein to dissociate from the receptor. The R-Smad is then able to bind to Smad4, and the complex translocate to the nucleus where it regulates transcription of specific target genes (Figure 1.6) [32, 33].

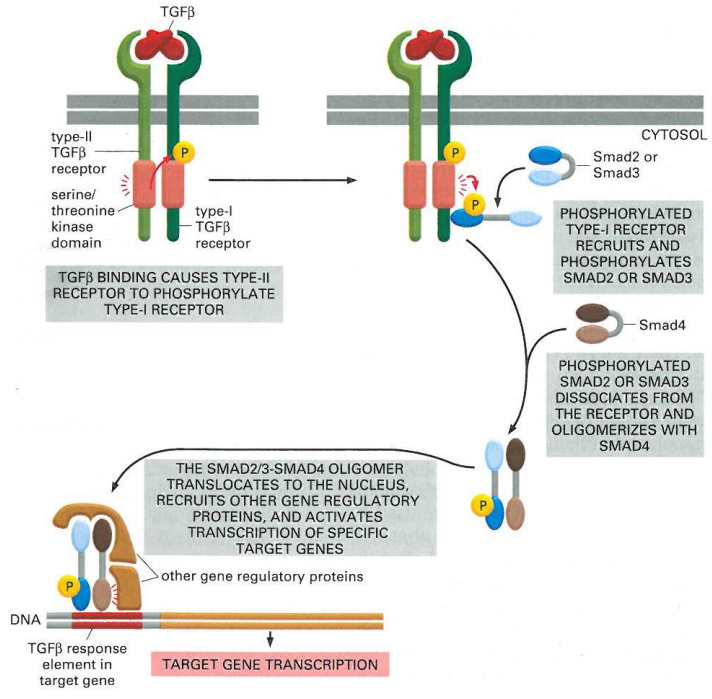

Figure 1.6 TGF-β activaded Smad signaling pathway. The image is adapted from Bruce Alberts' *Molecular Biology of The Cell* [32].

1.6 The S100-family

The S100 family consists of at least 21 small (10-12 kDa) calcium binding proteins with two Ca^{2+}-binding EF-hands [2]. The name S100 originates from the discovery made by *Moore, B. 1965* [34] that the members of this family was soluble in 100 % saturated ammonium sulfate [35]. The members of the S100-family do not possess any enzymatic activity, but obtain an essential conformational change when it binds Ca^{2+}. This conformational change exposes a hydrophobic interaction domain, making the S100 proteins able to recognize and bind to target proteins [2, 36]. The interaction of the S100-family proteins with a target protein may affect various biologic functions, including disease and inflammation, wound healing, stress response, cell motility, proliferation and differentiation [37].

Several of the family members have been identified in various types of cancer in association with proliferation and metastasis. Their occurrence is thought to have an indirectly prognostic value in the sense that the lower concentration of a S100-protein the patient have, the longer they will live [37]. S100A4 in particular has gained a lot of interest based on its metastasis-promoting nature [2], and as a marker of poor prognosis, especially in breast cancer [4, 5].

1.6.1 S100A4

S100A4 is located on chromosome 1q21 in a frequently rearranged gene cluster. Examples of normal cells expressing S100A4 are fibroblasts, macrophages, monocytes, T lymphocytes, neutrophilic granulocytes and endothelial cells [2]. An increasing degree of evidence state that S100A4, which has been identified in several tumors of different origins [38-42] and has proven to be associated with a poor patient prognosis [4, 5], might have an important role in EMT. Some of S100A4's biological functions include regulation of angiogenesis, cell survival, motility, and invasion, all important steps during metastasis [2]. Studies including *Davies, et al., 1993*, and *Grigorian, et al., 1996*, demonstrates that overexpression of S100A4 in benign and non-metastatic epithelial cells promoted acquisition of a metastatic phenotype as well as tumor growth, indicating that it plays a role in EMT [43, 44].

1.6.2 Intracellular S100A4

S100A4 has been detected in the nucleus, cytoplasm, and extracellularly. Most commonly, it is found in the cytoplasm where it primarily exists as a symmetric homodimer, facilitating binding of two homologous or heterologous target proteins [2]. Interaction of S100A4 and NMMHC (nonmuscle myosin heavy chain) IIA will increase the cells capability to migrate and thus give the cell a greater metastatic potential. In order for a cancer cell to move through tumor stroma, they have to degrade

some of the extracellular matrix components, a process facilitated by e.g. S100A4 mediated activation of certain MMP's [2].

The expression level of S100A4 in human cells depends primarily on methylation status, β-catenin and attribution from extracellular components. S100A4 is associated with transcriptional regulation of e.g. MMP's and E-cadherin, and some identified bindings partners include NMMHC IIA and IIB, actin, tropomyosin, p53, liprin β1, methionine aminopeptidase 2, CCN3, S100A1, p37 and septin 2, 6 and 7 (Figure 1.7 a). Most of these are yet to be confirmed target proteins in *in vivo* experiments, and their role in metastasis is thus mostly unknown [2].

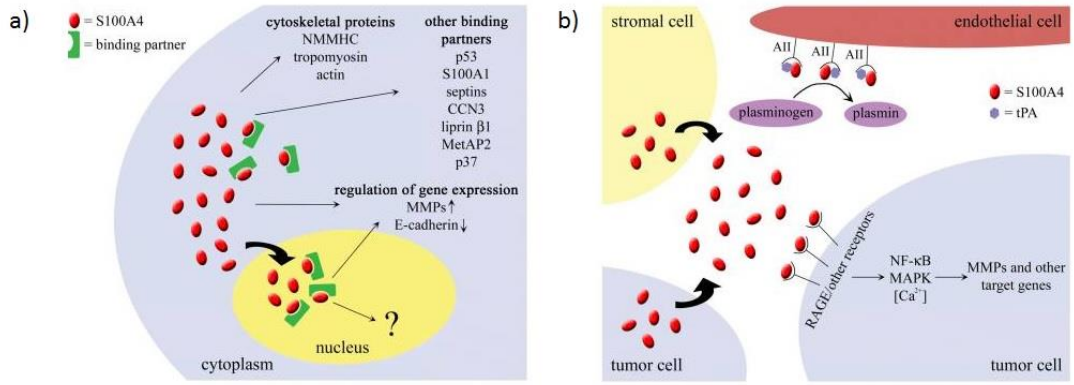

Figure 1.7 The figure illustrates binding partners and activity of S100A4 both intracellular (a) in the cytoplasm and nucleus, and extracellular (b). The figure is adapted from *Boye and Mælandsmo, 2010* [2].

1.6.3 Extracellular S100A4

Tumor cells, macrophages and fibroblasts have all been reported to secrete a multimeric form of S100A4 to the ECM, but the receptor activation by which the cell is stimulated to secrete is still unknown. Calcium activated extracellular S100A4 has been reported to bind to e.g. RAGE (receptor for advanced glycation end products) or other receptors, leading to the activation of downstream signaling pathways such as MAPK (mitogen-activated protein kinases) and NF-κB (Figure 1.7 b). Activated NF-κB result in downregulation of E-cadherin and upregulation of transcriptional markers such as Twist and Snail, as well as the mesenchymal marker vimentin. Activated signaling pathways results in regulation of several target genes involved in metastasis. Interaction of extracellular S100A4 with annexin II (AII) and tissue plasminogen activator (tPA) on the surface of endothelial cells have also been reported, converting plasminogen to plasmin resulting in promotion of angiogenesis [2, 36].

1.7 The HMLE model system

Primary human mammary epithelial cells (HMEC) may only be cultured for ~15 population doublings (PD) when cultured in MEGM medium (serum-free mammary epithelium growth medium). HMECs immortalized by retroviral-mediated expression of both the telomerase catalytic subunit hTERT (producing HMEC/hTERT cells) followed by SV40 large T and small t antigenes result in the HMLE cell line [26, 45]. The HMLE cell line is ideal for examination of the processes regulating EMT since the epithelial cells readily can undergo EMT. Furthermore, S100A4 expression is significantly upregulated in the mesenchymal cells [46]. The change in S100A4 expression is thus a good marker for induced EMT. The HMLE cell line used in this thesis was a kind gift from Robert A. Weinberg of the Whitehead Institute of Biomedical Research, Cambridge, MA, USA [26, 45].

Materials and Methods

2.1 Cell culture

The HMLE cells were cultured in a 1:1 mixture of serum-free Mammary Epithelial Cell Growth Medium (MEGM) (Lonza), and Dulbecco's Modified Eagle Medium: Nutrient Mixture F12 (DMEM/F12) (Gibco by Life technologies™). See Appendix 6.3 for complete list of supplements. This 1:1 mixture of the MEGM and the DMEM/F12 media is from here on out referred to as "complete growth media".

The HMLE cells were passed two to three times each week and incubated at 37°C with an atmosphere of 5 % CO_2. The cells were detached with Trypsin-Versene (EDTA) (Lonza), where 1 ml trypsin was added to a T25 bottle. The bottle was then incubated for approximately five minutes. To inactivate the trypsin, complete growth media was added to the cell suspension followed by a centrifugation at 1000 rpm for five minutes. The supernatant was discarded and the cell pellet was resuspended in complete growth media to achieve the right dilution. For experiments requiring the exact cell concentration, 10 µl of the cell suspension was mixed with 10 µl of Trypan blue stain (Gibco® by Life Technologies™) and applied to a Countess® cell counting chamber slide and analyzed on Countess® automated cell counter (both Invitrogen). For the TGF-β1 stimulation experiments, the cultures were treated with 3.3 ng/ml recombinant human TGF-β1 (R&D systems®).

The cells were frozen in a solution of 75 % complete growth media, 15 % fetal calf serum (FCS) and 10 % dimethyl sulfoxide (DMSO). When thawing the cells, the tube containing the cell suspension was placed in a 37°C water bath and immediately transferred to a T25 bottle with 5 ml warm, complete growth media. After eight hours, the media containing the dead, unattached, cells was replaced with fresh media.

This procedure is based on *Elenbaas et al.* publication from 2001 on HMLE and HMLER cells [45].

2.1.1 Mycoplasma test

The cell cultures were tested for mycoplasma on a regular basis, and found to be negative.

2.1.2 Immunomagnetic separation

To separate the epithelial cells form the mesenchymal cells, immunomagnetic separation (IMS) was used, and performed as described in *Tveito et al., 2011* [47]. The magnetic beads used was MOC31 (sheep anti-mouse) (Life Technologies™) and coated in-house with mouse anti-EpCAM, enabling binding of cells expressing EpCAM antigenes. EpCAM (epithelial cells adhesion molecule) is a cell surface marker found on epithelial cells. EpCAM-based IMS positively enrich for HMLE cells demonstrating an epithelial phenotype with low levels of S100A4. 1 ml cell suspension was mixed with 30 µl of the solution containing the MOC31 beads and incubated on a rotating rack at 4°C for 30 minutes. The beads with the epithelial cells and the cell suspension containing the mesenchymal cells were subsequently separated by using a magnet rack.

2.1.3 Incucyte™

The machine used for detection and monitoring of cell proliferation was the Incucyte™ FLR (Essen bioscience). The Incucyte™ FLR system allows live imaging of cultures, and enables both phase contrast and fluorescence microscopy through a fully automated compact microscope [48]. The Incucyte™ FLR is placed inside a regular incubator holding 37°C and with an atmosphere of 5 % CO_2.

The Incucyte test was performed to monitor the proliferation rate of the cell lines. The cells were cultured on a 96-well microtest™ plate (BD Falcon™) with a concentration of both 4 000 and 6 000 cells/well, and in parallels of 4 wells per cell line. The plates were placed in the Incucyte™ machine the day after seeding, and subsequently followed for 72 hours. Images were taken every two hours, and the cultures proliferation rate was estimated based on observed confluence. The software used to analyze the results was IncuCyte 2011A.

2.1.4 MTS assay

The MTS assay, also known as CellTiter96® AQ_{ueous} One Solution Cell Proliferation Assay (Promega), is based on colorimetric detection of viable cells in a culture for determination of e.g. proliferation. The CellTiter96® AQ_{ueous} One Solution reagent contain a tetrazolium compound (MTS) and an electron coupling reagent. The MTS compound will, in metabolically active cells (viable cells), be bioreduced to a colored formazam product by dehydrogenase enzymes. The electron coupling reagent ensures a stable solution when bound to the MTS compound. The quantity of formazan product measured in the culture is directly proportional to the number of living cells [49].

Cells were cultured on a 96-well plate with a concentration of 4 000 cells/well in parallels of four, as well as one well with complete growth medium (a blank) to subtract background absorbance. After 24,

48 and 72 hours, 20 µl of the CellTiter96® AQ_{ueous} One Solution reagent was added to the wells and the plate was incubated at 37°C for approximately 40 minutes before measurement of absorbance. After about 20 minutes of incubation, the plate was softly shaken to ensure an even color distribution.

Promega's protocol suggest that the absorbance should be measured at 490 nm. In the current study, the absorbance was measured at 560 nm on Modulus™ Microplate (Turner BioSystems). The change in measured absorbance was based on experiments previously performed at the Department of Tumor Biology.

2.2 Microscope techniques

2.2.1 Brightfield microscopy

All images were obtained using an Olympus IX81 microscope equipped with X-Cite® 120PC Q for immunofluorescence imaging.

2.2.2 Immunofluorescence

In order to study the cellular distribution of E-cadherin in the HMLE cells, immunofluorescence microscopy was performed. HMLE cells cultured on glass cover slips were incubated for three days, with or without stimulation with TGF-β1. The cells were washed with phosphate buffered saline (PBS) before fixation in 4 % paraformaldehyde (PFA) for 10 minutes in room temperature followed by a washing step using PBS. A subsequent incubation with PBS/glycine for 10 minutes was used to stop the fixation process. The fixated cover slips were stored in PBS at 4°C.

The cover slips were treated with 50 mM NH_4Cl for 15 minutes to further quench the effect of the PFA. For both washing and antibody dilution, 0.05 % saponin (solved in PBS) was used. The saponin was used to permeabilize the cell membranes. The cover slips were incubated with primary antibody anti E-cadherin (rat) clone DECMA-1 (abcam®) over night at 4°C in a humidification chamber, followed by three washing steps. Incubation with secondary antibody goat anti-rat (Invitrogen) labeled with TRITC as a fluorescent marker (excites at 557 nm) was performed in room temperature for 60 minutes, followed by three washing steps. The cover slips were mounted to SuperFrost® Plus objective glasses (Thermo Scientific) using ProLong® Gold antifade reagent with DAPI (Life Technologies™). Images were taken using identical exposure time for each fluorescent label.

2.3 Lentiviral transduction

To create a cell line lacking S100A4 expression, transduction with lentiviral particles containing shRNA against S100A4 was used. A shRNA is a small hairpin RNA that can be used for gene silencing via RNA interference (RNAi). In short, double-stranded DNA gets incorporated into a RISC (RNA induced silencing complex) which in turn is guided to the complimentary target mRNA. The shRNA regulates gene expression mainly through mRNA cleavage. The virus particles deliver the shRNA to the cell and make sure that it is integrated in the genome of the cell. The integrations will result in a stable downregulation of the target gene [50].

The HMLE cells were transduced with lentiviral transduction particles (Sigma-Aldrich). The transduction particles consists of lentivirus plasmid vectors containing a gene for both puromycin resistance and an anti-S100A4 shRNA. The addition of puromycin kills the cells who did not integrate the virus in its genome, and is thus referred to as a selection marker. The control virus has the exact same features as the actual virus, only lacking the anti-S100A4 shRNA. The control virus used for this transduction was MISSION® pLKO.1-Puro Non-Mammalian shRNA Control Transduction Particles (product nr: SHC002V) (Figure 2.1).

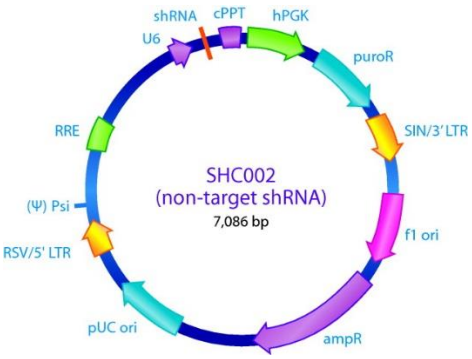

Figure 2.1 The MISSION® non-target shRNA control vector. The arrow labeled puroR represents the gene for puromycin resistance. The image is adapted from www.sigmaaldrich.com [51].

The anti-S100A4 virus used for the transduction was MISSION® shRNA Lentiviral Transduction Particles (product nr: SHCLNV-NM_002961). When performing a lentiviral transduction experiment for the first time, factors such as concentration of puromycin and hexadimethrine bromide (hexa) should be experimentally determined, as should the choice of MOI (multiplicity of infection). Experimental determination of the concentration of hexa is particularly important when working with non-cancerous cells such as the HMLE cell line. Optimization of both the concentration of hexa as well as the MOI enable the cells to take up as many virus particles as possible.

Because of the limiting time frame, the tests mentioned in the section above was not performed. All decisions were made on the basis of previously performed optimization experiments at the Department of Tumor Biology. It is also recommended to test several sh-viruses to choose the one that gives the best knock-down result. The Department of Tumor Biology has previously tested several anti-S100A4 viruses, and found the one used in the current study to have the best efficiency.

Prior to the application of the virus particles, 1 mg/ml hexa was added to the well with a final concentration of 8 µg/ml. An estimated volume of the virus particles were added to the wells containing hexa, and the cultures were incubated for 72 hours. After the incubation period, the media containing the virus particles was removed, and fresh media was added. Puromycin was added to the media to a final concentration of 2 µg/ml.

Table 2.1 Calculation of the volume to be used of both the control vector and the anti-S100A4 virus sample. The calculations are based on the first virus transduction.
TU = transduction particles/unit

Cell type	Cells seeded (number/well)	MOI	TU	Virus sample concentration	Estimated volume of virus sample
Epithelial shcontrol	12 500	5	12 500*5= 62 500	shctr: $2,8*10^7$ TU/ml	62 500 TU/$2,8*10^7$ TU/ml = 0,0022 ml = 2,2 µl
Epithelial shS100A4	12 500	5	12 500*5= 62 500	shA4: $1,6*10^7$ TU/ml	62 500 TU/$1,6*10^7$ TU/ml = 0,0039 ml = 3,9 µl
Mesenchymal shcontrol	25 000	5	25 000*5= 125 000	shctr: $2,8*10^7$ TU/ml	1250 000 TU/$2,8*10^7$ TU/ml = 0,0045 ml = 4,5 µl
Mesenchymal shS100A4	25 000	5	25 000*5= 125 000	shA4: $1,6*10^7$ TU/ml	125 000 TU/$1,6*10^7$ TU/ml = 0,0078 ml = 7,8 µl

The HMLE cells were cultured in a 24-well plate with different concentrations. The wells best fitted for the virus transduction contained, for the epithelial cells, 12 500 cells, and for the mesenchymal cells, 25 000 cells. The multiplicity of infection (MOI) is the number of transducing lentiviral particles per cell (TU/cell). In this experiment, a MOI of 5 TU/cell was used. The estimated volume of the virus samples used for each cell line is shown, with calculations, in Table 2.1. The reported titer of the anti-S100A4 shRNA was $1.6x10^7$, and the titer of control shRNA was $2.8x10^7$.

The virus transduction was performed twice. The numbers in Table 2.1 are from the first transduction. The second transduction was performed on the already transduced cells, using the same virus particles as the first time and the same MOI (5 TU/cell). 50 000 cells per cell line was used, resulting in a TU of 250 000. The estimated volume of the virus samples to be added were 9 µl for the control cell lines (shctr), and 16 µl for the anti-S100A4 cell lines (shA4) (calculation not shown).

2.4 Western blot and Immuno blot

2.4.1 Preparation of protein lysate

Lysis of the cells was performed by resuspending a frozen, dry cell pellet in 50 µl Radio Immuno Precipitation Assay buffer (RIPA) containing both phosphatase and protease inhibitors (contents in Appendix 6.3), and vortexed for five seconds. The cells were incubated for 60 minutes on ice, and vortexed every 15 minutes. To ensure further eruption of the cell membrane, the cells were sonicated for five seconds (using ultra sound waves), followed by 15 minutes of full speed centrifugation at 4°C. The supernatant was transferred to a new tube and stored at -70°C.

2.4.2 Measuring protein concentration

Protein concentration was measured by Pierce® BCA protein assay kit (Thermo Scientific). The procedure allows quantification of total protein in a sample based on colorimetric detection provided by bicinchoninic acid (BCA). The color reaction product is caused by the interaction of two BCA molecules and one cuprous ion (Cu^{+1}). This complex exhibit a strong absorbance almost linear with increasing protein in the sample (range 20-2000 µg/ml), and is detected at the wavelength of 562 nm.

The samples were pipetted in parallels to a 96-well plate. In order to determine the unknown concentrations, bovine serum albumin (BSA) (Thermo Scientific), was added to the plate at 9 different dilutions ranging from 25 to 2000 µg/ml, including a blank (0 µg/ml). The concentrations of the unknown samples were estimated based on the standard curve of the dilutions [52]. The measurements were performed on Modulus™ Microplate (Turner BioSystems).

2.4.3 Protein separation and gel blotting

For protein separation, the NuPAGE® Novex® Bis-Tris 4-12 % gel (NuPAGE® Midi Gel System) was used. The gel is a discontinuous SDS-PAGE system with neutral pH (7.0). The gel does not contain SDS. The running buffer used was NuPAGE® MES SDS. Prior to the application, the samples were mixed with NuPAGE® LDS sample buffer and NuPAGE® reducing agent and heated to 75°C for 10 minutes to ensure that the proteins were denatured and unfolded [53]. SeeBlue® Plus2 Pre-stained Standard was used as ladder. The electrophoresis was performed in XCell4 Surelock™ Midi-Cell, with PowerEase500 as power supply. All products mentioned in this section were produced by Invitrogen.

At the end of the electrophoresis, the separated proteins in the gel were blotted from the polyacrylamide gel to a nitrocellulose membrane using an iBlot® transfer stack. The blotting

procedure used was dry transfer method performed on a iBlot®-7 Minute Blotting System (Invitrogen).

2.4.4 Antibody incubation, exposure and detection

The method used for detection of protein expression of S100A4 was chemiluminescence. When horseradish peroxidase (HRP) and a peroxide buffer is mixed together, luminol is oxidized and forms an exited state product that emits light as it decays to its ground state [54].

The membrane was blocked in a 5 % milk powder solution solved in the R&D reaction buffer (Appendix 6.3). The primary antibodies, monoclonal anti-S100A4 clone 22.3 [55] or anti α-tubulin (Millipore), was added to a 2 % milk powder solution and incubated over night at 4°C with a dilution of respectively 1:500 and 1:5000. The secondary antibody, polyclonal rabbit anti-mouse (DAKO) conjugated with HRP, was also added to a 2 % milk powder solution and incubated for 60 minutes in room temperature with a dilution of 1:3000.

The solution used for development was SuperSignal® West Dura Extended Duration Substrate (Thermo Scientific), and was added to the membrane prior to the exposure with luminescence. The emitted light produced by the chemical reaction was detected on G:BOX (SynGene) and analyzed with GeneSnap software.

2.5 Flow cytometry

Flow cytometry is a technique that allows counting and analyzing of single cells or microscopic particles. A single cell flow suspension is passed through several lasers where factors such as size, granulation, and bound fluorochromes are detected. The size of the cell is determined by forward scatter (FSC) where the laser beam has an alteration of its angel between 5° and 30°. The granulation of the cell is determined by side scatter (SSC) where the laser has an angel alteration of 90° (Figure 2.2). To determine whether the cells express different cell markers, direct or indirect binding of antibodies labeled with fluorochromes are used. The laser will excite the fluorochrome and the emission light, as well as scattered light, is detected by photomultiplier tubes (PMTs) illustrated with the grey boxes detecting the lasers in Figure 2.2 (Flow). To eliminate the detection of both electronic and optical noise and ensure that the correct information from the scattered light and the fluorochrome emission is detected, the light is directed through mirrors and filters. These filters direct emission of different wavelengths to its respective PMT, enabling detection of several fluorochromes in one sample at the same time. The PMTs convert the detected light in to electric pulses that are sent to the

computer for analysis. The detected emission intensity is directly proportional to the number of fluorochromes in the sample [56].

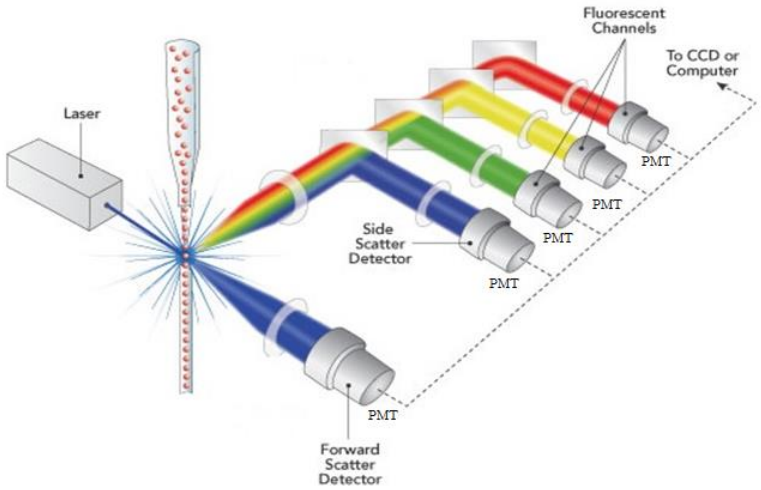

Figure 2.2 An illustration showing how the scattered light of the laser beam is directed through several mirrors and filters, directing the emitted light of different wavelengths to its respective PMT. The figure is adapted from www.semrock.com [57].

2.5.1 Sample preparation and detection

Cells used for these experiments were subcultured two days prior to analysis. The cells were detached as usual and resuspended in flow cytometry buffer, 60 µl per reaction tube needed of the current sample. The flow cytometry buffer contained 1 mg/ml γ-globulins from human blood (Sigma-Aldrich), solved in PBS. One reaction tube consisted of 60 µl cell suspension solved in flow buffer, as well as X µl of the antibody of interest, depending on dilution. The total volume of the antibody labeling solution was 120 µl, and flow buffer was added to obtain the correct volume. One reaction tube per cell line should always be unstained, as a control, consisting of 60 µl cell suspension solved in flow buffer as well as 60 µl plain flow buffer. Antibodies that have been used in the current study are listed Appendix 6.1 (Flow cytometry). The tubes containing the cells and antibodies were incubated at 4°C for 30 minutes followed by centrifugation at 1000 rpm for five minutes. The supernatant was carefully pipetted of and discarded, and 200 µl PBS was added to the tubes. This solution was filtered through a 35 µm filter to avoid clustering of cells. Just prior to analyzing the samples, 1 µl Hoecst 33258 (Sigma-Aldrich) was added to separate living and dead cells in the sample. The machine used in the current study was the BD LSR II Flow Cytometer (Becton Dickinson Bioscience), analyzed by FlowJo_V10.0.5.

2.6 Reverse transcription quantitative PCR (RT-qPCR)

2.6.1 RNA purification

The RNA purification was performed using QIAshredder™ and RNeasy® Mini Kit (both QIAGEN), on dry, frozen cell pellets. The spin columns consists of a silica-based membrane with selective binding properties. A high-salt buffer system allows up to 100 µg of RNA longer than 200 bases to bind the silica-membrane.

The frozen cell pellet was resuspended in a RLT buffer mixed with β-mercaptoethanol (10 µl in 1 ml RLT buffer) for lysis and homogenization of the sample. The β-mercaptoethanol is added when purifying RNase-rich cell lines. The RLT buffer contains highly denaturing guanidine-thiocyanate which immediately inactivates RNases to ensure purification of intact RNA. To make sure that the lysis and homogenization of the sample was sufficient, the sample was vortexed or pipeted prior to the application to the QIAshredder spin column. The spin column was centrifuged and 1 volume of 70 % ethanol was added to the flow-through. The addition of ethanol provides appropriate binding conditions. The flow-through mixed with ethanol was applied to an RNeasy spin column where total RNA binds to the silica-membrane and contaminants are discarded with the flow-through. The flow-through was from here on out discarded after centrifugation, all but in the last step. Following the addition of 70 % ethanol was the application of RW1 buffer to the RNeasy spin column, and subsequently addition of RPE buffer. In the last step, the RNA was eluated with RNase-free water that broke the bindings to the silica membrane. The RNA lysate was then frozen and stored at -70°C [58].

2.6.2 RNA quantification

RNA concentration was measured by NanoDrop™ 2000 (Thermo Scientific), a small spectrophotometer that enables the measurement of either nucleic acids or proteins based on the measurement of absorbance. The absorbance of RNA concentration was measured at a wavelength of 260 nm and the concentration was given in µg/µl [59].

2.6.3 c-DNA synthesis

In order to study the RNA lysates by quantitative polymerase chain reaction (qPCR), a DNA copy of the messenger RNA (mRNA) had to be made. The transformation of mRNA to complimentary DNA (c-DNA) using RNA-dependent DNA polymerase enzyme is termed reverse transcription. A primer exploiting the poly-A tale of the mRNA binds to the mRNA in the sample, a process the reverse transcriptase enzyme is dependent on for DNA synthesis [60]. A reverse transcription PCR might be performed as a one-step or a two-step qPCR. In one-step qPCR the reverse transcription and qPCR is

performed in the same tube. In the two-step qPCR, which was used in the current study, the transcription of c-DNA and the qPCR reaction is performed in two separate tubes [61].

A c-DNA synthesis kit (qScript™ cDNA Synthesis kit by Quanta Biosciences) containing both reverse transcriptase and a reaction mix as well as nuclease free H_2O was used to produce c-DNA. 1 µl of the qScript™ Reverse Transcriptase solution and 4 µl of the qScript™ Reaction mix (5x) was added to each sample. Based on the measured concentration of RNA in the samples, estimations were made to find the volume to be taken out of the sample to obtain a solution with a concentration of 1 µg. Nuclease free H_2O was added to gain a final c-DNA synthesis solution with a total volume of 20 µl. The c-DNA synthesis program was performed on GeneAmp® PCR System 9700 with a program composed of 5 minutes at 25°C, 30 min at 42°C, and 5 min at 85°C, before the samples were cooled down to 4°C. An additional volume of 80 µl were added to the samples before storage at -20°C.

2.6.4 Quantitative PCR

Real-time or quantitative PCR (qPCR), allows the detection of a given amplification product, an amplicon, as the reaction progresses (real-time), with quantification after each cycle. In contrast to conventional PCR, qPCR allows determination of the initial number of template copies, and is therefore both qualitative (presence or absence of a sequence) and quantitative (copy number) [61]. The qPCR protocol used in this work consisted of 2 different stages repeated through 40 cycles. First, the sample was heated to 95°C for three minutes, denaturing the c-DNA. The denaturing step dissolves double-stranded DNA to single-stranded DNA, which are then used as templates in the next step. The second step was annealing and elongation at 60°C (one minute), where the forward and reverse primers with target gene specific sequences as well as the fluorescence labeled probe binds to the templates, enabling new strand synthesis. The heat-stabile Taq DNA polymerase, derived from the *Thermus aquaticus* bacteria [62], binds to the primers on the template, generating a double stranded product. As the sample was heated back up to 95°C, the new, double stranded product was denatured, creating two templates. When the PCR reaction is in its exponential phase, as illustrated in Figure 2.3, each cycle generates a doubling of the previous cycle's amount of templates, and the fluorescence detected is proportional with the amount of amplicon. The change in detected fluorescence over time is used to calculate the amount of amplicon after each cycle. As the reaction proceeds, some of the components needed to produce a new template will run out, and the reaction enters the plateau phase [62].

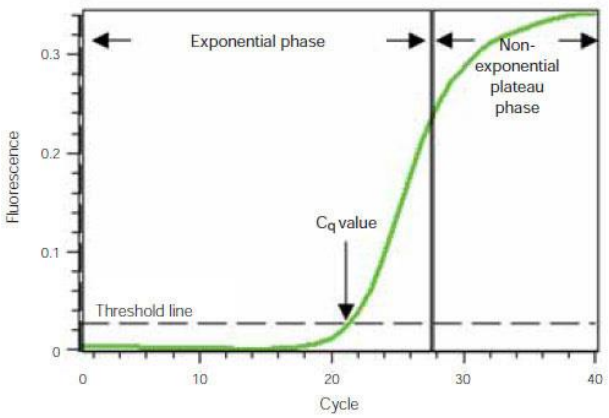

Figure 2.3 The figure illustrates the two phases of a qPCR reaction, both exponential and non-exponential phase, with the x-axis showing the number of cycles and the y-axis showing the fluorescence form the amplification reaction. The figure is adapted from www.bio-rad.com [61].

The principle for detection is termed fluorescence resonance energy transfer (FRET). The probe consist of two molecules, a fluorescent labeled reporter and a quencher. When kept close together, as they are when the probe is intact, the quencher will decrease the fluorescent intensity of the reporter by absorbing the reporters emitted photon (Figure 2.4). Once the Taq DNA polymerase starts constructing a new strand of DNA from the template, during elongation, it will eventually meet the probe, which is bound to the template. The Taq DNA polymerase possess exonuclease activity, which enables cleavage of the probe. The reporter is released from the inhibiting power of the quencher, and fluorescent signal is detectable. This principle prevents emission of fluorescent signals from unbound probes [62].

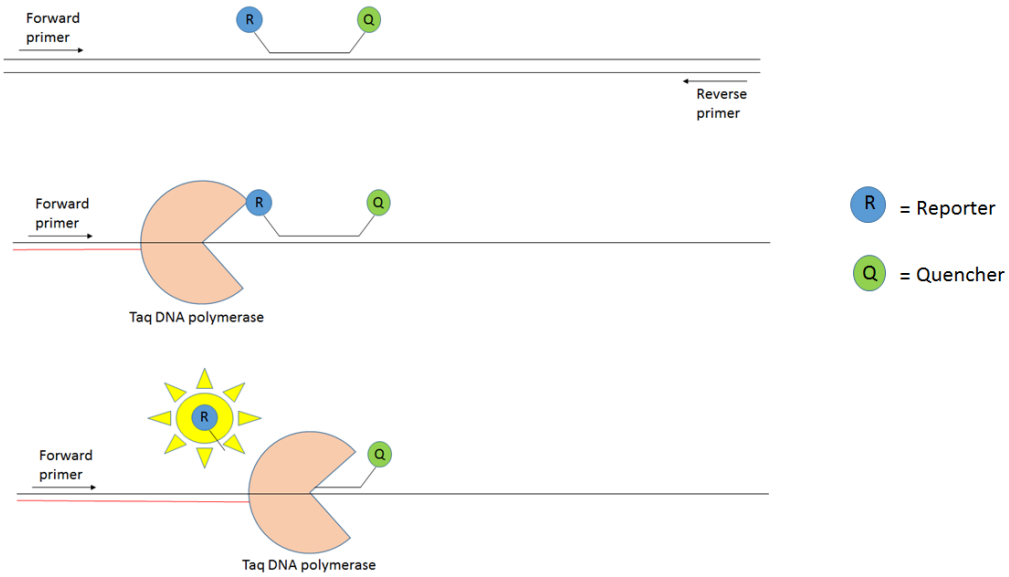

Figure 2.4 Taq DNA polymerase with exonuclease activity, releasing the reporter from the quencher.

When the qPCR reaction initially starts, it uses some cycles to reach a detectable amount of produced fluorescence that exceeds the background fluorescence signal. The measurement is made in the exponential phase of the reaction where all components are surplus, and enables reliable and accurate calculations of the initial amount of template in the sample. In the example of Figure 2.3, this is at cycle 21, and is called the quantification cycle or C_q value. If the initial amount of template is high, the sample will need fewer cycles to reach a reliable C_q value than if the initial amount of template is low [61].

The analysis of the samples was performed by addition of 25 µl per well in parallels to an iQ™ 96-well PCR plate (Bio-Rad). One sample consisted of 5 µl c-DNA mixed with 2.4 µl primer/probe mix, 7.6 µl H_2O and 15 µl PerfeCTa® qPCR SuperMix (Quanta Biosciences). The SuperMix contains all components needed for the qPCR reaction, with the exception of primer/probe mix and c-DNA. A key component of the SuperMix is AccuStart™ Taq DNA polymerase with monoclonal antibodies attached to it, as well as the four deoxynucleoside triphosphates needed for DNA synthesis. The antibodies attached to the DNA polymerase keeps it from being active prior to the first denaturing step, where the antibodies denature irreversibly, releasing fully active, unmodified Taq DNA polymerase [63]. The primer/probe mix comprised of 0.9 µl of both forward and reverse primers, mixed with 0.6 µl probe, resulting in a total volume of 2.4 µl.

The experiments in the current study was performed on BioRads iCycler™ and post-run data was analyzed using iCycler and Genex. A list of the primers and probes used in these experiments can be found in Appendix 6.1 (RT-qPCR).

2.7 Statistics

All experiments performed during the current study was performed twice unless else is stated. TGF-β1 treatment of the epithelial HMLE cell line was performed four times. One biological parallel was discharged due to equal levels of S100A4 mRNA in the epithelial cultures, both the shctr and shA4. The standard deviation is indicated with error bars (Figure 3.13 and 3.14), when three biological parallels was measured.

Results

3.1 Characteristics of the HMLE cell line

To enable elaboration of the question in this thesis' aim, it was necessary to create a cell culture model system where S100A4 was not expressed. The HMLE cell line [45] was ideal for this purpose. As previously stated, the model system consist of both epithelial and mesenchymal cells. HMLE cells can, when exposed to various stimuli [46, 64], change between an epithelial and a mesenchymal state. The HMLE cells are able to spontaneously differentiate into the other cell type (spontaneous EMT/MET). This can be controlled by carefully culturing. A major issue throughout this work has been to monitor and control spontaneous drift in the cell system.

In order to overcome the problem of the drift in the cell system, and to obtain as pure populations as possible, immunomagnetic beads labeled with anti-EpCAM was used to separate HMLE cells in EpCAM positive (epithelial) and EpCAM negative (mesenchymal) cells. Figure 3.1 illustrates the morphology of the HMLE cell line after IMS with MOC 31 coated beads.

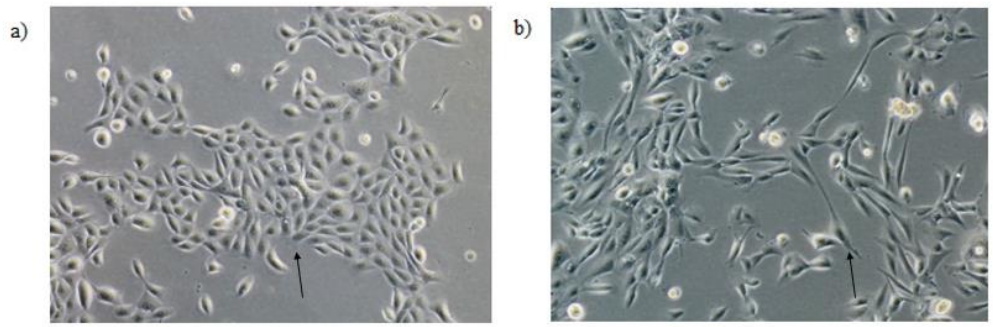

Figure 3.1 IMS separated HMLE cells using EpCAM as a selection marker. Images are taken with 10x magnification. a) EpCAM positive cells. The arrow points to a cluster of cells with typical epithelial morphology. The cells are small, cubical, and grow close to their neighbor cell, forming cobblestone like islands in the culture flask.
b) EpCAM negative cells. The arrow point to a typical mesenchymal HMLE cell. The cell is elongated, pointy and grows in distance from the nearest neighbor. When the culture becomes confluent, the mesenchymal culture will resemble fibroblasts. In this particular image, a mix of mesenchymal and epithelial HMLE cells are evident.

3.1.1 Validation of the IMS procedure

In order to keep the percentage of epithelial cells at a steady level, the morphology of all the cultures were monitored every second day throughout the experiments, and the epithelial cultures was subjected to IMS before setup of experimental series. It was therefore of interest to validate the effectiveness of the IMS procedure, especially before the lentiviral transduction was performed. Presence or absence of CD44, CD24 and EpCAM on the cell surface has previously been published as biological markers for the HMLE cell line [46, 65]. Both the EpCAM positive and EpCAM negative HMLE cell population was therefore analyzed by flow cytometry staining for EpCAM, CD24 and CD44 (Figure 3.2), and in addition characterized on protein and mRNA level (Figure 3.3). EpCAM and CD24 are biological markers mostly expressed on epithelial cells, while CD44 is mostly expressed in mesenchymal cells. The result in figure Figure 3.2 a and c confirmed the epithelial version to be mainly $CD44^{-}/CD24^{+}$. Among the mesenchymal, EpCAM negative cells on the other hand, a much higher percentage had of $CD44^{+}/CD24^{-}$ and $CD44^{+}/EpCAM^{-}$ expression (Figure 3.2 b and d).

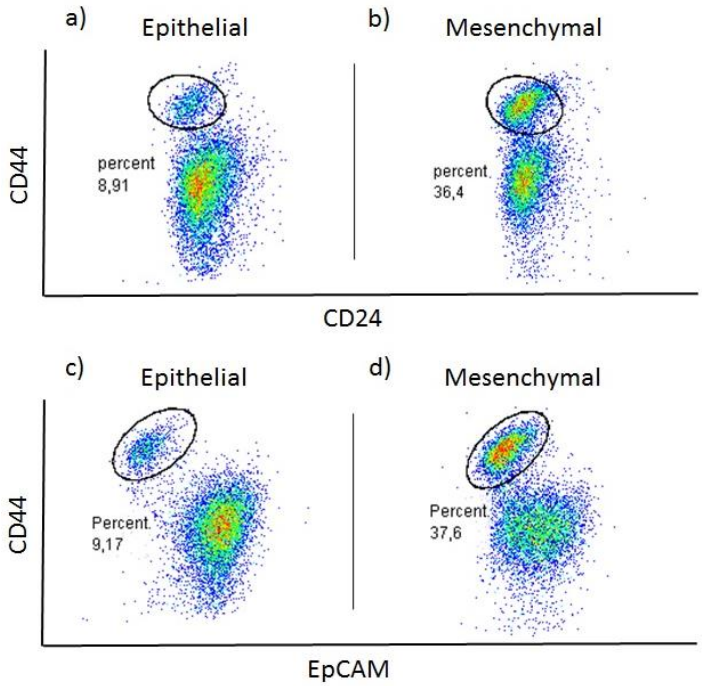

Figure 3.2 Flow cytometry using EpCAM, CD24 and CD44 antibodies. a-b) $CD44^{+}/CD24^{-}$ is gated. c-d) $CD44^{+}/EpCAM^{-}$ is gated. The $CD44^{+}$ cells are gated to illustrate the part of the population that, according to *Mani et al., 2008* and *Morel et al., 2008*, possess mesenchymal characteristics [26, 65].

S100A4 is stated to be a biological marker of mesenchymal status of the HMLE cells [2, 3, 46]. This was confirmed by both western blot (Figure 3.3 a) and RT-qPCR (Figure 3.3 b). The expression of S100A4 mRNA was three times higher in the mesenchymal cell population (Figure 3.3 b) than in the epithelial cell subpopulation. The difference in S100A4 and N-cadherin mRNA levels (Figure 3.3 b) between epithelial and mesenchymal cells was clear and in line with differences previously described

[26], and would probably have been even clearer if the two distinct subpopulations had been even better separated than shown in Figure 3.2 b and d.

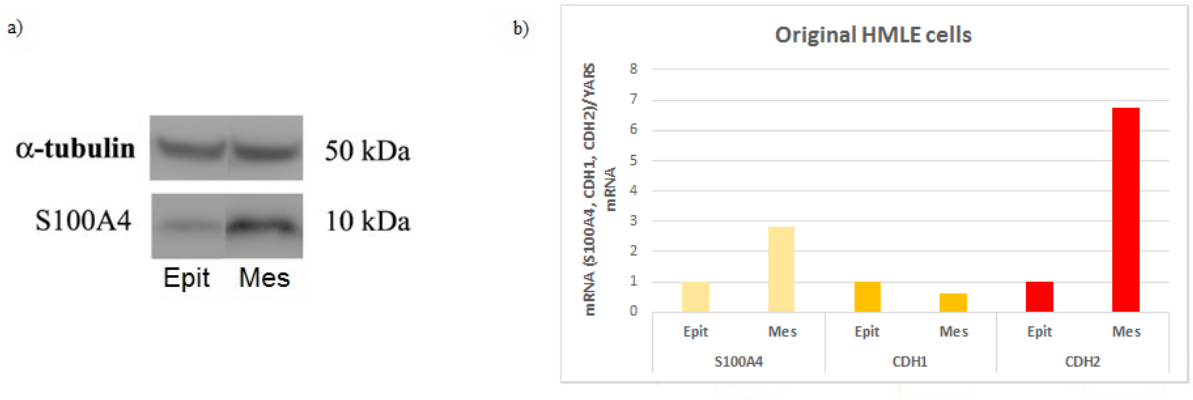

Figure 3.3 a) Western blot showing expression of S100A4 in epithelial (Epit) and mesenchymal (Mes) cells. b) mRNA level of S100A4, CDH1 encoding E-cadherin and CDH2 encoding N-cadherin, illustrating the relative fold difference in mRNA expression between epithelial and mesenchymal cells. It does not say anything about actual difference in mRNA expression in the samples. The epithelial sample was used for normalization, and the fold change is estimated based on this.

3.2 Knock-down of S100A4 in epithelial and mesenchymal HMLE cells

3.2.1 Lentiviral transduction

In order to decipher the role of S100A4 during EMT, HMLE cell lines lacking S100A4 expression was made using lentiviral transduction. S100A4 was expressed at low levels in the epithelial cells, but showed significant expression in the mesenchymal version of HMLE cells (Figure 3.3 a).

3.2.2 Morphology of the transduced cells

The introduction of the virus particles created 4 new cell lines. Epithelial shcontrol (Epit shctr), mesenchymal shcontrol (Mes shctr), epithelial shS100A4 (Epit shA4) and mesenchymal shS100A4 (Mes shA4). The two latter are the S100A4 knock-down cell lines. As expected, the epithelial cell lines showed no morphologic difference between the cell lines transduced with the shctr and shA4 virus particles. Both the epithelial transduced cell lines resembled the EpCAM positive original HMLE cell cultures (Figure 3.1 a vs. Figure 3.4 a and b). The mesenchymal shctr (Figure 3.4 c) showed no evident morphologic difference from the EpCAM negative HMLE cells (Figure 3.1). The mesenchymal shA4 did, however, show an altered morphology resulting in a super "mesenchymal-looking" culture (Figure 3.4 d).

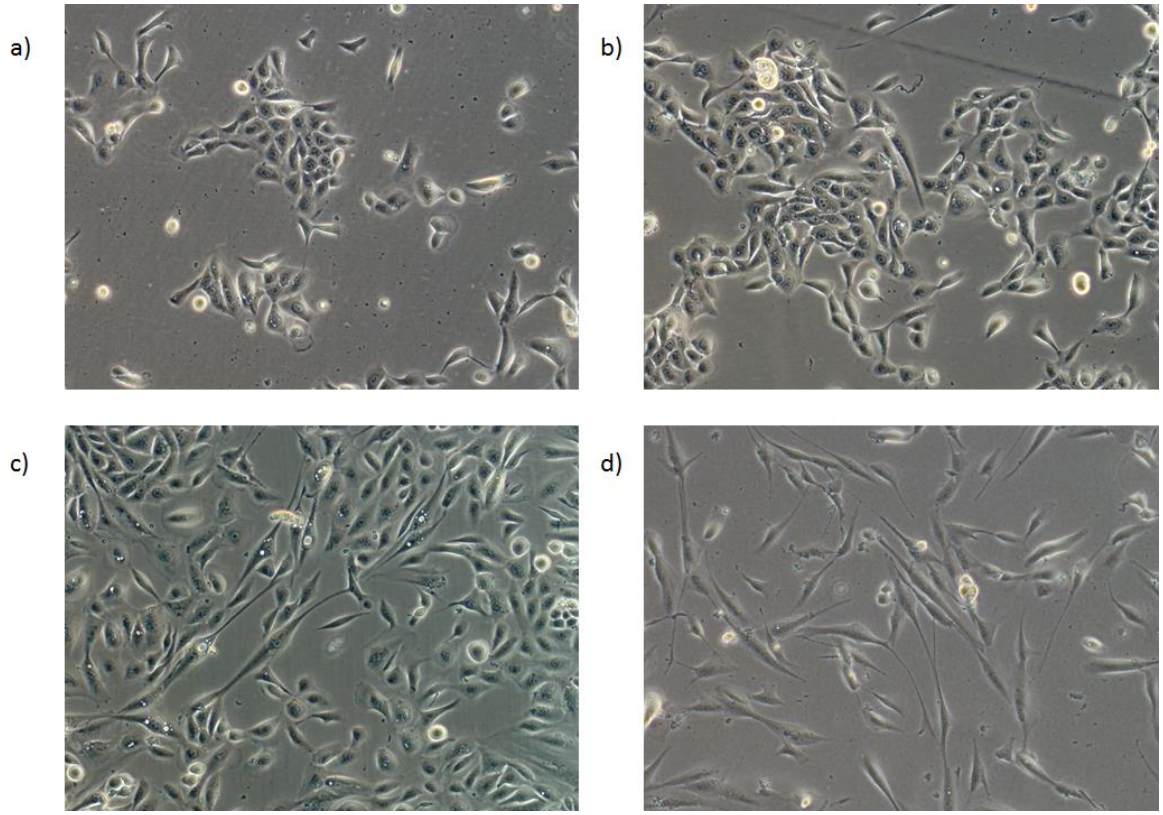

Figure 3.4 Morphology of the cell lines with (shA4) and without (shctr) S100A4. a) Epithelial shctr. b) Epithelial shA4. c) Mesenchymal shctr. d) Mesenchymal shA4. Images was taken with 10x magnification.

3.2.3 Expression of S100A4 and mesenchymal markers in transduced HMLE cells

Western blot was used to control the degree of knock-down of S100A4 (Figure 3.5) in the two cell lines treated with the anti-S100A4 virus (shA4). The knock-down of S100A4 was not satisfying, especially in the mesenchymal shA4 culture. It was therefore decided to do an additional transduction on the already transduced cell lines, of both shctr and shA4. Prior to the second virus transduction, IMS was performed to enrich for the mesenchymal, EpCAM negative cells. The results in chapter 3.2 and 3.3 are all based on cell from the second virus transductions unless otherwise stated.

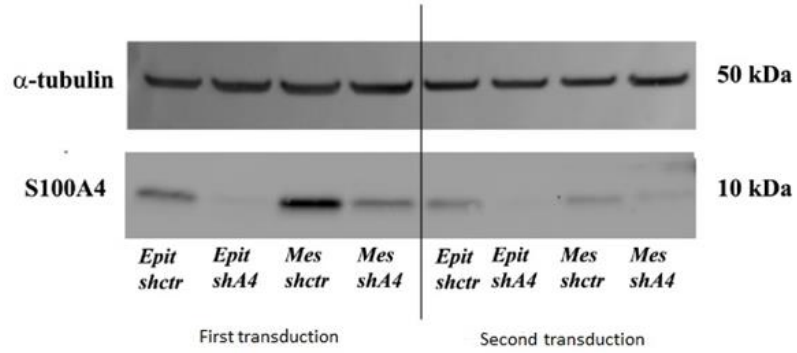

Figure 3.5 Western blot showing S100A4 protein expression after the first virus transduction and second transduction. α-tubulin was used as loading control.

Figure 3.5 shows that both transductions reduced the level of S100A4 protein expression significantly. The level of S100A4 in the mesenchymal shctr seemed surprisingly low, but the loading control indicated that less protein lysate was loaded in that well than what was loaded of the epithelial shctr. In addition, the flow cytometry of negative selected EpCAM-IMS cells indicated that this population could have been even more enriched for mesenchymal cells (Figure 3.2). To control for the stability of the S100A4 knock-down, RT-qPCR was performed on the epithelial shctr and shA4 cells after each experiment, using S100A4 primers (Figure 3.6). The S100A4 expression was turned back on after long term culturing of the epithelial shA4 cells (results not shown), and experiments were the fold difference in S100A4 mRNA expression was smaller than 3 was not included in this thesis.

Figure 3.6 illustrates the relative fold difference in mRNA expression of S100A4, CDH1 encoding E-cadherin and CDH2 encoding N-cadherin between shctr and shA4. The relative expression of S100A4 decreaseed in both epithelial and mesenchymal shA4, indicating a successful knock-down.

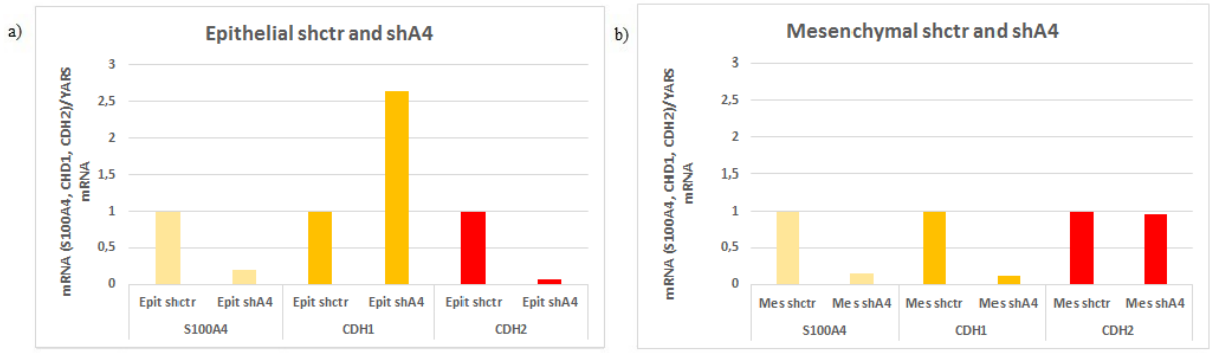

Figure 3.6 mRNA level of S100A4, CDH1 and CDH2. a) Epithelial shcontrol (Epit shctr) was used for normalization and fold difference was estimated based on this.
b) Mesenchymal shcontrol (Mes shctr) was used for normalization and fold difference was estimated based on this. The bars in the two graphs are normalized against different values and shows relative expression. The height of the bars represented in both a and b are thus not comparable between the two.

The relative mRNA expression of E-cadherin and N-cadherin in both the epithelial and mesenchymal cell cultures illustrates the change in the cell lines' expression pattern when lacking S100A4. When examining E-cadherin, it may seem as though the epithelial shA4 cell line become even more epithelial, while the mesenchymal shA4 cells become more mesenchymal. The levels of N-cadherin on the other hand seems to remain stable in the mesenchymal cell lines, and decreasing in the epithelial cell lines, emphasizing that the epithelial shA4 cells become even more epithelial when lacking S100A4. This result is contradictory to the results found by flow cytometry (Figure 3.7 and 3.8).

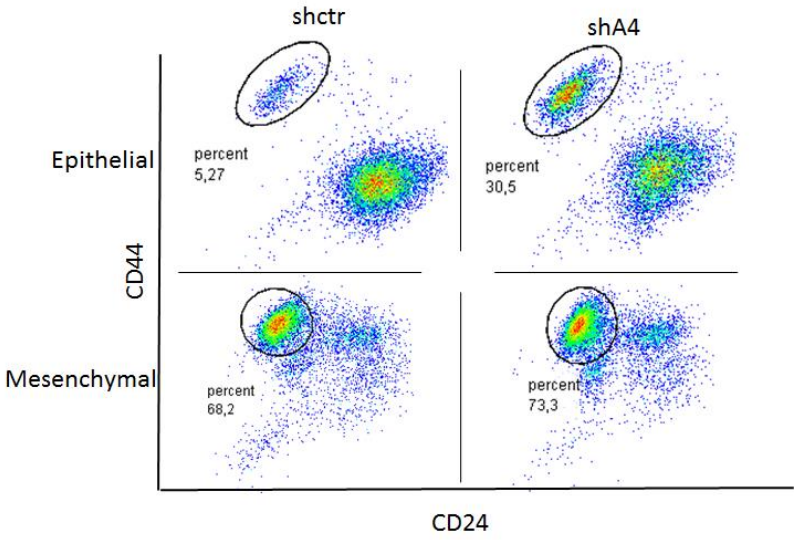

Figure 3.7 Flow cytometry using EpCAM, CD24 and CD44 antibodies. $CD44^+/CD24^-$ is gated to present the percentage of the total amount of cells possessing mesenchymal characteristics.

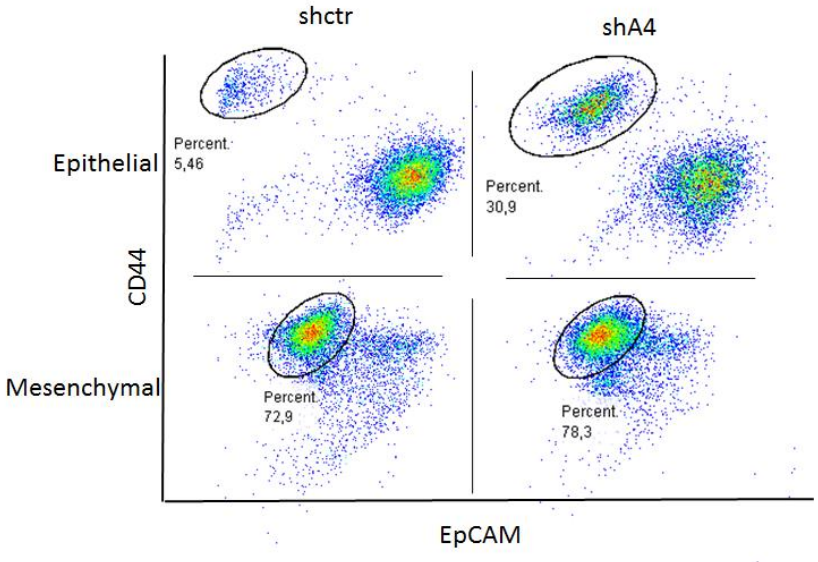

Figure 3.8 Flow cytometry using EpCAM, CD24 and CD44 antibodies. $CD44^+/EpCAM^-$ is gated to present the percentage of the total amount of cells possessing mesenchymal characteristics.

It was also of interest to test whether elimination of S100A4 influence the expression of CD24, CD44 and EpCAM on the cell surface. Both the $CD44^+/CD24^-$ and $CD44^+/EpCAM^-$ plots showed approximately the same results. In the epithelial cells, knock-down of S100A4 seemed to make the cells more mesenchymal with a percentage rising from about 5 % to 30 %. This result was in strict contradiction with results shown earlier (Figure 3.4 a and b and Figure 3.6 a). In the mesenchymal cultures, the percentage of $CD44^+$ was much higher in both shctr and shA4 than what was shown in the original HMLE cells (Figure 3.2). This was probably due to the IMS cleanup of the culture before the second virus transduction. The knock-down of S100A4 did not, however, seem to affect the cell

surface markers in any extent with numbers of about 70 % in shctr and about 75 % in shA4, indicating that the change in morphology seen in Figure 3.4 c and d was not caused by change in expression of CD24, CD44 and EpCAM.

3.2.4 Proliferation of the transduced cells

When observing the cell lines, the epithelial cell lines, both shctr and shA4, seemed to have a more rapid proliferation than the mesenchymal cell lines. It was therefore of interest to establish whether the knock-down of S100A4 affected the cells proliferation. To verify these observations, both Incucyte™ and MTS assay was performed. The Incucyte assay measures proliferation rate by continuous still photos of the well containing the cells. However, because the mesenchymal cells are larger than the epithelial cells, the wells containing the mesenchymal cells would tend to fill the well as rapid as the epithelial cells. These results were thus not representative for measurement of proliferation (results not shown).

The results from the MTS assay gave a better indication of the proliferation rate of the different cell lines. Figure 3.9 shows the growth curve made on the basis of three different experiments where the standard deviation in the results is shown with error bars. The absorbance was measured at 560 nm on Turner Modulus™ Microplate (BioSystems) after 24, 48 and 72 hours. In order to study any difference between the cell lines proliferation rate, the samples were normalized against the absorbance measured after 24 hours for each cell line. There seemed to be a trend that the shA4 cell lines had a less rapid proliferation than the shctr cell lines (not statistically tested).

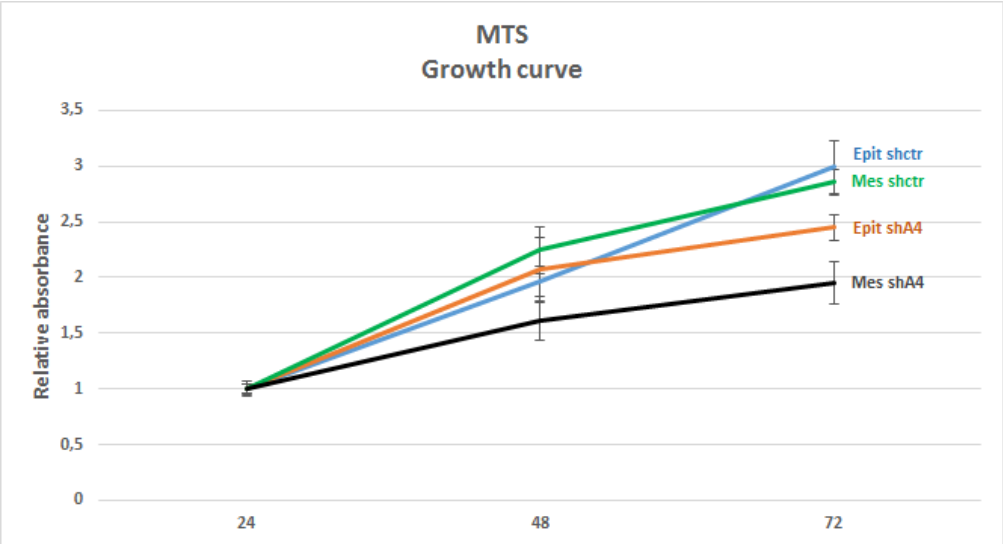

Figure 3.9 MTS growth curve showing relative absorbance between the different cell lines.

3.3 TGF-b1 induced EMT

In order to study whether the HMLE cells would be able to induce EMT without S100A4, the cells were experimentally stimulated with TGF-β1. TGF-β1 has previously been shown to induce EMT in HMLE cells [65]. Evaluation of a change from expressing epithelial markers to mesenchymal markers was observed through monitoring of cell morphology, mRNA expression of biological markers associated with EMT, as well as cellular distribution of E-cadherin. For these experiments, only epithelial cells were used since the mesenchymal cells already express mesenchymal markers. TGF-β1 stimulation was performed four times where the amount of cells and days of stimuli was optimized. Surprisingly, in the epithelial shctr cells of the three first experiments, the level of S100A4 was lower after TGF-β1 treatment compared to the non-stimulated cultures (Figure 3.14 a). This was highly unexpected and it was hypothesized that this was caused by over-confluent cultures.

In the fourth experiment the cultures were split to avoid the cultures from becoming confluent. The expression of S100A4 was virtually the same in both the epithelial shctr and shA4 (Figure 3.10). It is was thus not possible to make any indications about possible changes in the biological markers tested with RT-qPCR, and the result was discarded.

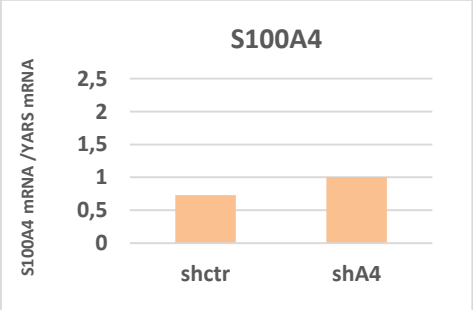

Figure 3.10 qPCR results showing fold difference in S100A4 expression between non-stimulated epithelial shctr and shA4 from the fourth experiment.

The subsequent results presented are representative figures from the first three experiments.

The phase contrast images from the TGF-β1 stimulation experiments (Figure 3.11) illustrates the change in morphology observed during the time of stimulation compared to non-stimulated epithelial cells of both shctr and shA4. Images obtained after one day of stimuli did not portray any big differences, but a few cells of both shctr and shA4 seemed to have gained mesenchymal characteristics. After six and eight days of stimulation, an alteration in the cells morphology had become more prominent, and several cells of both the shctr and shA4 cultures had gained mesenchymal characteristics.

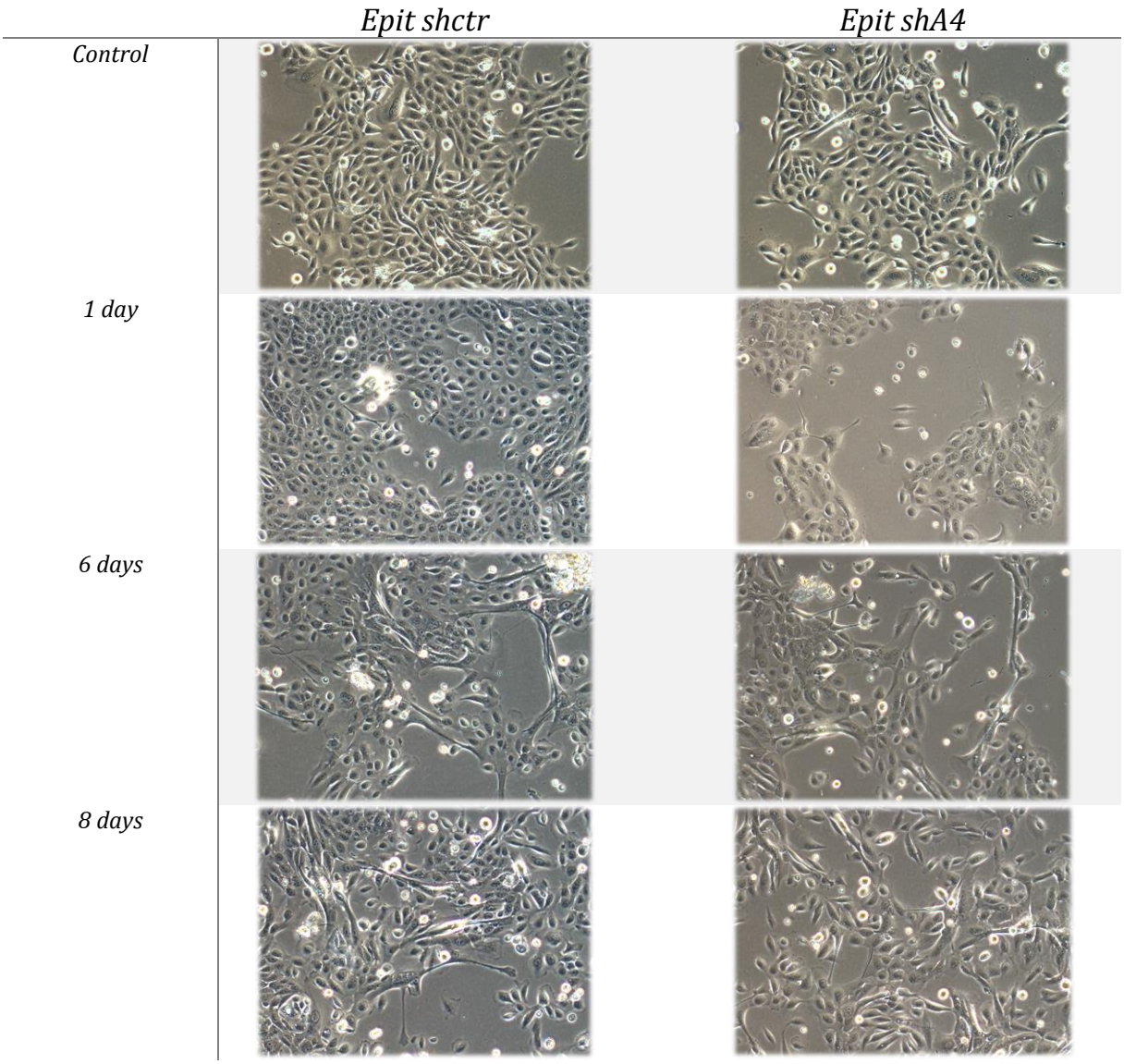

Figure 3.11 Phase contrast images of representative cultures,10x magnification.

E-cadherin expression is known to be affected by both S100A4 expression and during the process of EMT, and the distribution of this cell surface adhesion molecule was investigated by immunofluorescence staining of TGF-β1 stimulated (three days) and non-stimulated cultures (Figure 3.12).

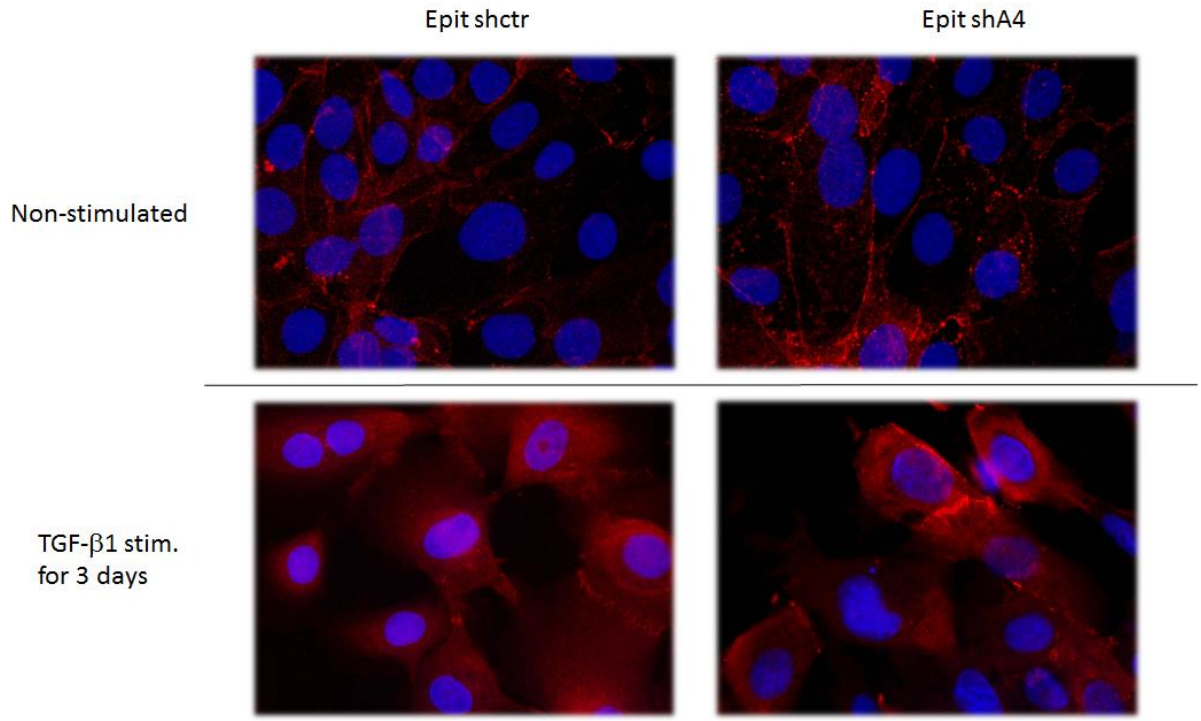

Figure 3.12 Cover slips with immunofluorescence staining. Stained with DAPI (nuclear color, blue) and anti-E-cadherin (TRITC-red).

In the non-stimulated epithelial cells, E-cadherin seemed to be distributed mainly in the cell membrane, while E-cadherin seemed to be "smeared" evenly throughout the cell after stimulation with TGF-β1, indicating that TGF-β1 treatment affected the distribution of E-cadherin in the cells. This pattern was observed in both the shctr and shA4 cells. There was no evident difference between the cell lines, indicating that TGF-β1 mediated E-cadherin redistribution was not dependent on S100A4 expression.

In order to study whether knock-down of S100A4 had any impact on the mRNA expression of several biological markers, RT-qPCR was performed. The biological markers of interest was S100A4, CDH1, CDH2, vimentin, SNAI1/2 and ZEB1/2.

Before the examination of the biological markers was performed, the relative expression of S100A4 in epithelial shA4 compared to shctr was controlled. Figure 3.13 show that the difference between shctr and shA4 was adequate for comparison of the other markers.

Figure 3.13 qPCR results showing fold change difference in S100A4 expression between non-stimulated epithelial shctr and shA4. The graph shows the average of three experiments. The error bar illustrate the standard deviation of the fold difference between epithelial shctr and shA4 cells.

Figure 3.14 b shows the alteration in the biological markers through the course of TGF-β1 stimulation compared to a non-stimulated culture (on the left side in the graphs) for both epithelial shctr and shA4. The graphs illustrates relative fold difference in mRNA expression of CDH1, CDH2, vimentin, SNAI1/2 and ZEB1/2 in relation to the reference gene YARS.

The TGF-β1 stimulation experiment was performed three times. Only six days of stimulation was measured in all three experiments, and the bar representing relative expression after six days is thus the only one with an error bar. The results after one and eight days of stimulation was measured in two experiments.

The relative expression of CDH1 in both shctr and shA4 as well as SNAI1 in shctr did not seem to be affected by the TGF-β1 stimulation when compared to the non-stimulated culture. The bar representing one day of stimulation in SNAI1 was most likely a false result caused by the sensitivity of RT-qPCR, and needs to be repeated. Considering that the bars at six days and eight days of stimulation did not pose any big difference from the non-stimulated culture, the likelihood that the bar from one day of stimulation is a false result was relatively high. SNAI2, ZEB1 and ZEB2 seemed to be increased. CDH2, however, seemed to have the biggest alteration in expression pattern with a 90 and 37 fold induction after eight days of stimulation in the epithelial shctr and shA4 respectively when compared to the non-stimulated culture. An increase in CDH2, a mesenchymal marker, together with no significant difference in HMGA2 (results not shown) indicated that TGF-β1 can induce EMT in both shctr and shA4 epithelial cultures. Therefore, the epithelial HMLE cells can undergo TGF-β1 induced EMT in the absence of S100A4 expression.

a)

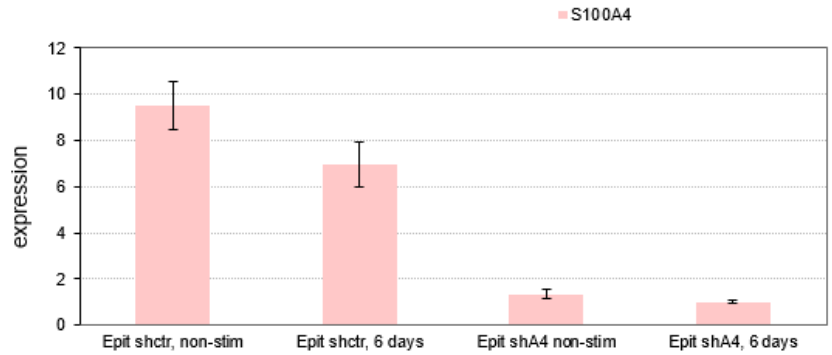
S100A4
expression
12
10
8
6
4
2
0
Epit shctr, non-stim
Epit shctr, 6 days
Epit shA4 non-stim
Epit shA4, 6 days

b)

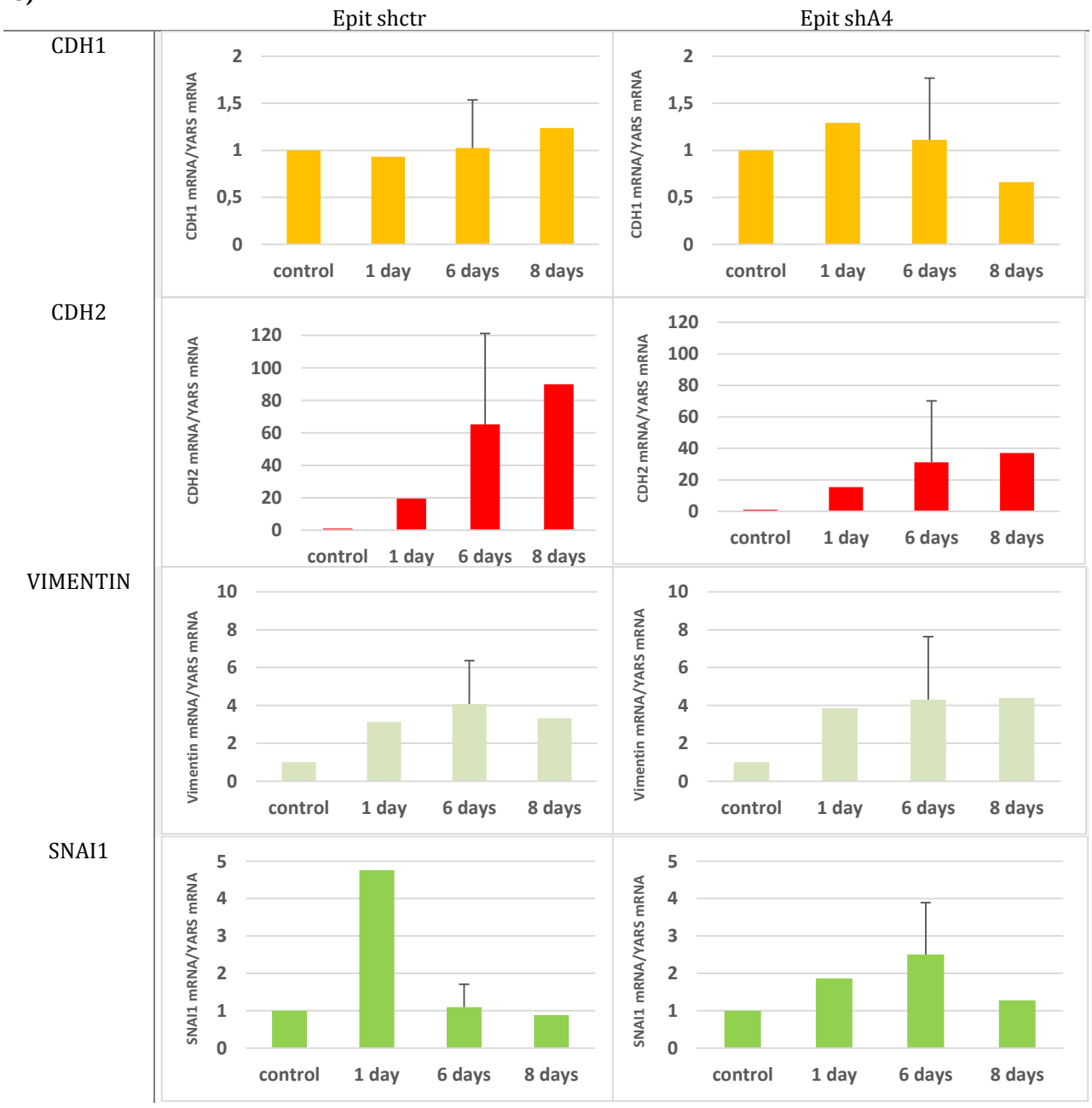
Epit shctr
Epit shA4
CDH1
CDH2
VIMENTIN
SNAI1
CDH1 mRNA/YARS mRNA
CDH2 mRNA/YARS mRNA
Vimentin mRNA/YARS mRNA
SNAI1 mRNA/YARS mRNA
control
1 day
6 days
8 days

SNAI2

ZEB1

ZEB2

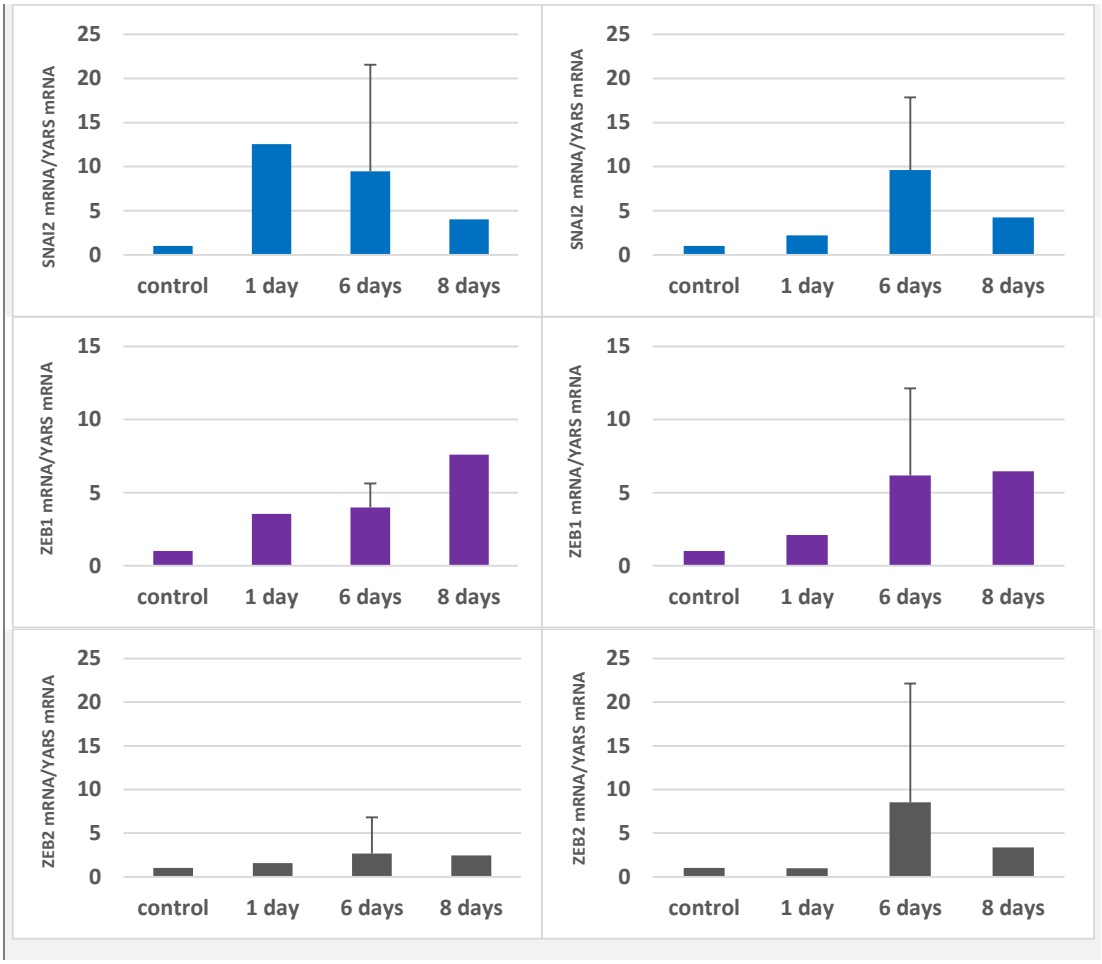

Figure 3.14 a) Representative graph of S100A4 RT-qPCR on TGF-β1 stimulated epithelial cell lines. The graph represents one of three experiments with similar results.

b) RT-qPCR results of 7 biological markers associated with EMT illustrated with relative amount of biological marker in relation to relative amount of reference gene (YARS), shown with fold difference.

Note that the scaling on the y-axis varies between the graphs.

Discussion

The aim of the study was to investigate whether an immortalized human mammary epithelial cell line lacking S100A4 expression would be able to undergo EMT. For this purpose, the HMLE cell line was chosen. S100A4 is mainly expressed in the mesenchymal cell type and expressed in a very small amount in the epithelial cell [26, 46]. S100A4 has through several studies been established as a biological marker of mesenchymal status, and has thus been used to detect carcinoma cells that have undergone EMT [2, 3].

4.1 The role of S100A4 during EMT induction

To enable elaboration of whether the epithelial cells of the HMLE cell line could undergo EMT without the presence of S100A4, S100A4 was knocked down using lentiviral transduction with anti-S100A4 shRNA. Only the epithelial cells from the virus transduction was used in the TGF-β1 stimulations experiments to induce EMT since the mesenchymal cells already express mesenchymal markers. The epithelial cell lines were subsequently stimulated with TGF-β1 for eight days. The experiments enabled comparison of non-stimulated with TGF-β1 stimulated cells, both shctr and shA4.

Evaluation of whether the two epithelial transduced cell lines had undergone TGF-β1 induced EMT was done by monitoring cellular morphology, measurement of mRNA expression of EMT related genes, and by monitoring the cellular distribution of E-cadherin. Evaluation of the morphological change observed (Figure 3.11) indicated that both the shctr and shA4 cultures were able to gain mesenchymal characteristics. There was no evident difference in the morphological response to TGF-β1 between the two cell lines, indicating that the absence of S100A4 did not affect the induction of EMT, as measured by change in morphology.

The gene expression of mesenchymal markers was also evaluated on the basis of relative mRNA expression of CDH1, CDH2, vimentin, SNAI1, SNAI2, ZEB1, ZEB2 and S100A4, all biological markers associated with EMT.

Previous studies have shown that the expression of both N-cadherin and vimentin is elevated when mammary gland epithelial cells or carcinoma cells have undergone EMT, while the expression of E-cadherin is decreased [26, 65]. When evaluating the results of the current study (Figure 3.14 b), both

CDH2 and vimentin seemed to increased. These data are in line with results presented by *Morel et al., 2008*, where stimulation of the HMLE cell line with TGF-β1 for eight days caused an increase in vimentin expression [26], suggesting that the EMT was indeed induced in our cultures. Furthermore, SNAI2, ZEB1 and ZEB2 expression was also increased in both shctr and shA4. For SNAI1, a trend where the expression was somewhat increased in the shA4 compared to the shctr cells was observed. However, the difference in expression was due to large variations in the results, and thus not significant. Further elaboration of the markers in relation to S100A4 expression is needed to conclude on this difference.

A trend where the majority of the EMT markers changed after TGF-β1 stimulation indicated induction of EMT in both cell lines, and that the absence of S100A4 did not affect the cells ability to undergo EMT. Interestingly, the mRNA expression of E-cadherin seemed to be unaffected by the TGF-β1 treatment. Since E-cadherin has been reported to be a central molecule in the regulation of EMT, and cells undergoing EMT are reported to lose E-cadherin mediated cell-cell contact, this was somewhat surprising. It was therefore of interest to investigate whether the intracellular distribution of E-cadherin changed during TGF-β1 stimulation [26, 65].

Both shctr and shA4 cells were cultured on glass cover slips and stimulated with TGF-β1 for three days. As shown in Figure 3.12, the non-stimulated shctr and shA4 both showed a distribution of E-cadherin mainly in the plasma membrane and between the cells, a typical epithelial phenotype. Knowing the role of E-cadherin as an adhesion molecule keeping epithelial cells together in an epithelial sheet, this distribution was as expected. The distribution pattern of E-cadherin seemed to change in both shctr and shA4 when the cells were stimulated with TGF-β1, which might indicate that E-cadherin is redistributed during EMT. This result strengthen the assumption that TGF-β1 stimulation successfully induced EMT, regardless of S100A4 expression in the epithelial HMLE cells.

4.1.1 Efficiency of S100A4 knock-down

The EMT induction experiment was performed four times where it was experimented with different amounts of cells, as well as the number of days of stimulation. In the fourth experiment, the cells were detached and reseeded every third day to prevent the cultures from becoming too confluent, a situation observed in the first three experiments. This was done to study whether confluence affected the expression of the biological markers tested with RT-qPCR. Unfortunately, when evaluating the difference in S100A4 mRNA expression (Figure 3.10) between the non-stimulated shctr and shA4 cells from the fourth experiment, the fold difference was less than 0.5, and it actually indicated that the levels were higher in the shA4 cells than in the shctr cells. This result may indicate that the expression

of S100A4 had been turned back on in the knock-down cell line, and the results from the fourth experiment was thus not used.

Evaluation of the relative mRNA expression of S100A4 between shctr and shA4 in the three previous experiments (Figure 3.13) indicated that the fold difference of S100A4 was sufficient to allow comparison of the cells dependency of S100A4 for EMT.

4.1.2 Variation in gene expression data obtained by RT-qPCR

The three experiments the results are based upon were performed without detachment of the cells. The cultures were as a consequence confluent (100 %). This might have had an impact on the expression pattern of the biological markers. However, all the cultures were treated under identical conditions, and the differences observed were considered to not be a result of the confluence.

Since the stimulation experiments were performed with different numbers of days under stimulation only the six days time point was repeated enough times to perform statistics and giving error bars (Figure 3.14 b). The deviation observed in the error bars might be a result of the varying degree of confluence observed in the three different experiments, as well as the sensitivity of RT-qPCR.

Even though one and eight days of stimuli only were tested twice, the trend observed from one to eight days of stimuli gives a good indication of the alteration in expression pattern.

4.2 HMLE cells as a model system for EMT induction

The HMLE cell line was selected for this thesis based on previously published work where the cells ability to induce EMT, when one or several genes associated with EMT has been knocked down, has experimentally been tested. As examples, both *Onder et al., 2008* and *Gupta et al., 2009* used shRNA to inhibit expression of human CDH1 to gain better understanding of E-cadherins role for induction of EMT. Introduction of anti-CDH1 shRNA generated a bigger proportion of HMLE cells who had gained mesenchymal characteristics [46, 64].

4.2.1 Stability of the model system

Throughout the work with this thesis there has been somewhat of a challenge culturing the HMLE cells. HMLE was chosen as a suitable cell line based on the epithelial cell's ability to undergo EMT and gain mesenchymal characteristics, and hence expression of S100A4. Immunomagnetic beads (IMS) coated with anti-EpCAM was used to separate the two populations in respectively EpCAM

positive (epithelial) and EpCAM negative (mesenchymal) cells. Questions were raised whether EpCAM alone was sufficient to claim "purity" of the distinct populations. It was shown that the $CD44^+$ expressing population (cells with mesenchymal characteristics [26, 65]) overlaps with the EpCAM negative population, which supports EpCAM as a selection marker dividing the two populations.

Trying to keep the two distinct populations separate was difficult, especially the mesenchymal population. For some reason, these cells continuously drifted back to express epithelial characteristics. This might have occured as a response to environmental factors. *Sánchez-Tilló et al., 2012* show that maintenance of a mesenchymal state requires cooperation between external stimuli, such as transforming (TGF-β), fibroblast (FGF), epithelial (EGF), insulin-like (IGF), hepatocyte (HGF), and platelet-derived (PDGF) growth factors, as well as estrogens, Wnt, Shh (sonic hedgehog), inflammatory cytokines, hypoxia, and, in the case of cancer progression, oncogenes [20]. In the current study, the cells were cultured under fairly defined conditions, using growth medium without serum, but with supplements (EGF, insulin, hydrocortisone), that might have positively enriched for the growth of epithelial cells.

Before IMS, the HMLE cell lines contained a mix of epithelial and mesenchymal cells. IMS was therefore performed prior to some experiments to enrich the cultures of the cell type of interest. Even IMS separated cells which had been cultured only a few passages indicated that the epithelial and mesenchymal populations comprised of a mix of the two cell types. Optimally, this procedure should have been performed strictly prior to all experiments to ensure a good distinction between the two cell populations. Factors that might have influenced the effectiveness of the IMS may be the amount of immunomagnetic beads used was too small compared to the amount of cells to be separated. This could have been solved by supplementary amount of beads. Another solution might have been to perform further IMS in the EpCAM negative cell suspension to gain a better selection for mesenchymal cells. A test to establish whether EpCAM in comparison to other biological markers would result in the best separation could also have been performed.

Despite the not fully optimized analyzing conditions, the purity of the epithelial population was satisfying to the extent that the TGF-β1 stimulation experiments could be performed.

4.2.2 Choice of mesenchymal markers

The most common mRNA expression markers used for determination of mesenchymal status are N-cadherin, vimentin and fibronectin, as described by Onder and Gupta [46, 64].

In other studies performed on the HMLE cell line, including *Morel et al., 2008* and *Mani et al., 2008,* cells with mesenchymal characteristics has been identified by fluorescence-activated cell sorting (FACS) using CD24 and CD44 as markers. The different populations identified in the HMLE cell line was one with a majority of $CD44^-/CD24^+$ as well as $CD44^-/EpCAM^+$ (from here on out referred to as $CD44^-$), which identified cells with epithelial characteristics, while $CD44^+/CD24^-$ and $CD44^+/EpCAM^-$ (referred to as $CD44^+$) populations identified cells with mesenchymal characteristics [26, 65]. In an article published by *Al-Hajj, et al., 2004,* the distinction between tumorigenic and non-tumorigenic breast cancer cells derived from a tumor was characterized by their $CD44^+$ expression pattern, where the $CD44^+$ was the most aggressive. [66].

When examining the HMLE cell line, *Morel, et al., 2008* identified 1.4 % of the cells to be $CD44^+$. After retroviral-mediated expression of H-Ras^{V12} of the cell line, generating the HMLER cell line (with increased oncogenic potential), followed by sorting of $CD44^-$ and $CD44^+$ cells, $CD44^-$ cells were cultured to enable isolation of single cells. After three weeks, 35 individual clones were isolated for characterization. The results showed that 47 % consisted of only $CD44^-$ cells, 33 % consisted of both $CD44^-$ and $CD44^+$, and 19 % consisted of only $CD44^+$ cells, demonstrating that $CD44^+$ mesenchymal cells can originate from $CD44^-$ epithelial cells (through e.g. EMT) [26]. This might also explain the difficulties in keeping the epithelial HMLE cells of the current study purely epithelial.

The flow cytometry plots presented under results in this thesis show the percentage of the cell populations that, according to Mani and Morel, possessed mesenchymal characteristics, both CD44+/$CD24^-$ and $CD44^+/EpCAM^-$.

Based on these publications and similar studies, the determination of mesenchymal status in the current study's cell lines were in part determined by the mRNA expression pattern of S100A4, CDH1 and CDH2 obtained by RT-qPCR, in addition to flow cytometry, using CD24 and CD44, as well as EpCAM as markers.

4.3 Effects of lentiviral transduction using anti-S100A4 shRNA

The western blot presented in Figure 3.5 compared the protein expression level from the first lentivirus transduction with the second transduction. S100A4 is normally expressed at very low levels in epithelial cells. The relatively high level of S100A4 expression in the epithelial shctr sample from the first virus transduction might be explained by the relatively high percentage of cells who possessed mesenchymal characteristics in the epithelial culture shown in the flow cytometry plot of the HMLE cells pre-transduction presented in Figure 3.2. These results indicated that about 10 % of the epithelial

population possessed mesenchymal characteristics, which further explained the continuous drift in the model system. S100A4 also seemed to be equally expressed in the epithelial shctr and in the mesenchymal shA4, which should not be expressing S100A4, after the first transduction. Based on these results, the cultures were IMS separated prior to a second virus transduction. The subsequent results showed that the extent to which S100A4 had been knocked down in both epithelial and mesenchymal shA4 was satisfying. The cells from the second virus transduction were used in all subsequent experiments.

After the second lentivirus transduction the morphology of shctr and shA4 of both epithelial and mesenchymal were compared. Figure 3.1 illustrates the morphology of the IMS separated, non-transduced HMLE cells. When comparing these images to the images taken after the lentiviral transduction (Figure 3.4), the epithelial cultures of both shctr and shA4 posed no evident morphologic difference either between the two of them or to the original non-transduced culture. This indicated that knocking down S100A4 did not result in a morphologic alteration, and neither did the introduction of a vector to the cells genome. The mesenchymal shctr culture showed great resemblance to the non-transduced mesenchymal population, indicating that the introduction of a vector did not cause any morphologic alteration. The mesenchymal shA4 population on the other hand seemed to generate a population featuring even greater mesenchymal characteristics than the non-transduced and the shctr, indicating that the mesenchymal shA4 became even more mesenchymal when lacking S100A4. This result was surprising, but organization of the cytoskeleton is important for the cell shape, and S100A4 expression has been associated with reorganization of the cytoskeleton [67]. It is therefore interesting to speculate whether the observed change in the cell shape of the mesenchymal cells of the HMLE cell line, both shctr and shA4, might be a result of restructuring of the cytoskeleton as a response to loss of S100A4, especially since the biological cell surface markers CD24, CD4 and EpCAM was unaffected by S100A4 status.

The flow cytometry results acquired of the non-transduced HMLE cells, both epithelial and mesenchymal (Figure 3.2), illustrated a drift in the HMLE model system as previously mentioned. IMS had not been performed strictly prior to the analysis, which is evident in the plots presented in Figure 3.2. Cells possessing mesenchymal characteristics are shown both in the plot representing CD44/CD24 and CD44/EpCAM, and they both showed approximately the same percentage distribution. The results indicated that about 9 % of the cells of the claimed epithelial population possessed mesenchymal characteristics, while only about 37 % of the mesenchymal population were truly mesenchymal. One source of error could have been that not enough antibodies were added to the solution, but since both the CD44/CD24 and CD44/EpCAM figure showed the same result, this was not likely.

Flow cytometry was also performed after the lentivirus transduction to evaluate whether the cells distribution pattern remained stable, or if introduction of a vector alone or knock-down of S100A4 resulted in any alterations. Both the plot representing CD44/CD24 (Figure 3.7) and CD44/EpCAM (Figure 3.8) showed approximately the same percentage distribution. IMS was performed prior to the lentivirus transduction, but not strictly prior to the flow cytometry analysis. Despite this, there seemed to be a better selection between the epithelial shctr and mesenchymal shctr than what was the case for the non-transduced cells (Figure 3.2). The only factor that separated these cultures from the non-transduced cells was the introduction of a control vector providing puromycin resistance. The percentage of cells who possessed mesenchymal characteristics in the epithelial shctr population was about 5 %, indicating that there still was a mix present, but to a much lower extent than what was observed in the non-transduced population. The mesenchymal shctr population comprised of about 70 % of cells with true mesenchymal characteristics, which was a huge improvement from the non-transduced cells where only 37 % were truly mesenchymal. This might come as a result of the IMS performed prior to the lentivirus transduction. The same pattern was observed in the mesenchymal shA4 population with a percentage of about 75 %, which indicated that knocking down S100A4 did not result in any alteration in the distribution of the current markers, and the observed change in cell shape did not affect the expression of CD24, CD44 or EpCAM on the cell surface.

When the epithelial shctr and shA4 populations were compared, the percentage of cells who possessed mesenchymal characteristics increased from about 5 % to about 30.5 %. The cells was treated under otherwise similar conditions, which indicated that it most likely came as a result of knocking down S100A4. This suggested that the epithelial cells actually started to express mesenchymal markers to a greater extent when they no longer expressed S100A4. This observation contradicted what was observed morphologically, were both the epithelial shctr and shA4 (Figure 3.4 a and b) looked identical. This also contradicted what was observed in the cells mRNA expression pattern (Figure 3.6 a). To further investigate whether these results reflected what actually happened in the HMLE cells when S100A4 was knocked down, all the experiments need to be performed again.

This result, and the results from the mesenchymal shctr and shA4, indicated that there was little or no correlation between the morphology of the cells and the expression of cell surface markers observed with flow cytometry.

The result from the RT-qPCR on the epithelial cells illustrated that the relative expression of CDH1 was increased with a 2.5 fold when S100A4 was knocked-down, as well as the relative expression of CDH2 which was decreased with about 1 fold. These results indicated that the epithelial cells lacking S100A4 acquires an even more epithelial phenotype. The relative expression of the EMT markers in the mesenchymal shctr and shA4 populations indicated, however, that the cells lacking S100A4

acquired a less epithelial phenotype when the bars in Figure 3.6 b which represented CDH1 was evaluated. The mesenchymal shA4 was decreased about one fold in their E-cadherin expression compared to shctr. The levels of CDH2 on the other hand seem to be stable, perhaps suggesting that an already high expression level could not be increased further. However, the mRNA expression of these genes were only analyzed in two separate samples, and a third test might have elucidated whether the alterations observed were biologically significant.

Both Incucyte™ and MTS assays was performed to monitor the proliferation rate of the different cell types in relevance to each other. Incucyte™ proved not to be a good method for the HMLE cell line, and the results where thus discarded. The growth curve that portrayed the relative proliferation of epithelial shctr and shA4, as well as mesenchymal shctr and shA4 was presented in Figure 3.9, and indicated that the cells with S100A4 knock-down grew a little less rapid than the shctr cell lines. However, this was not statistically tested. The difference in growth rate could possibly have explained why S100A4 expression was turned back on in the epithelial cultures after long term culturing. The cells expressing S100A4 will have a selective growth advantage, and eventually dominate the culture. This could also have explained why the difficulties in keeping the mesenchymal cultures purely mesenchymal, as the mesenchymal shA4 cells grew slower than the epithelial shA4 cells.

4.4 Metastatic ability, more than induction of EMT

Several studies, including publications from *Mælandsmo et al., 1996, Tabata et al., 2009, Fujiwara et al., 2011, Zhang et al., 2011,* and *Dahlmann et al., 2012,* has been performed to investigate the role of S100A4 in various cancer cells from different origins. Findings reported in these articles indicated that knocking down S100A4 caused suppression of cell migration *in vitro,* as well as reduced ability to metastasize and colonize [38-42]. It has been suggested that cells with S100A4 knock-down has less potential to undergo EMT, since cells who have undergone EMT usually has increased migration capability, as well as increased metastatic potential, a phenotype closely associated with S100A4 expression. The findings of this work contradicted the notion that S100A4 exerts its metastatic promoting role through induction of EMT.

It is, however, important to consider that the migration capacity, as well as the ability to metastasize and colonize, was not tested in the HMLE S100A4 knock-down cells in the current study. It would have been of great interest to do so, but unfortunately, the limited time available for research made this impossible to accomplish. Had there been more time, tests such as migration and invasion assays in Boyden chambers would have been performed.

4.5 Conclusions

Based on the presented results of the experiments executed during the work with this thesis, it seemes as though the HMLE cell line was an appropriate cell line to study the effects S100A4, and the lack of it, in induction of EMT in epithelial cells. The results indicated that the HMLE cells did not depend on expression of S100A4 to undergo EMT, based on the observed change in morphology as well as the change in the mRNA expression pattern of several biological markers associated with EMT induction. The results also indicate that the virus transduction was successful, leading us to believe that the experiments performed in the current study was successful.

4.6 Future perspectives

The time span of the thesis ranged from the beginning of August 2012 until May 2013. The short amount of time available limited the amount of tests to be executed. As a result, several questions remain unanswered. The future plans of what would have been done had there been more time are thus multiple.

For starters, some of the experiments were only performed twice. The key experiments, however, were performed three times. I would have liked to perform all test at least three times to get a better validation of the results. I would also have liked to further perform several TGF-β1 stimulation experiments to better enable visualization of a trend in the alterations observed in the EMT associated markers on an mRNA expression level. It would have been of great relevance to set up the experiments with controlled confluence to rule out that any alterations observed is a consequence of the degree of confluence. Lower levels of S100A4 mRNA after TGF-β1 stimulation and EMT induction could be caused by overly confluent cell cultures. It would also have been interesting to examine the protein level expression of S100A4 in the lentiviral transduced cultures after eight days of TGF-β1 stimulation.

Previous studies that have been performed on cell lines lacking S100A4 have all been tested to see whether the cells capacity to be motile and invasive changed as a result of the knock-down of S100A4, in addition to experiments showing change in mRNA expression patterns and morphology. Future perspectives to the current study will thus include both motility and invasion assays. In the current study, only the epithelial population of the HMLE cell line was used to study the cells ability to undergo EMT without S100A4. This was done based on the fact that the mesenchymal cells already express mesenchymal markers. Had there been more time, it would have been of great interest to examine whether knock-down of S100A4 could have impacted the already mesenchymal cells ability

to be motile and invasive through invasion and motility assays, and also what caused the change in cell shape caused by S100A4 knock-down. An experiment to examine the transduced HMLE cells response to reintroduction of S100A4 would also have been very interesting. This could have been tested by exposing the cells to recombinant S100A4 (rS100A4), or overexpressed mouse S100A4 mRNA as the cells have shA4 against human S100A4.

Previous studies where S100A4 have been knocked down have also observed changes in the expression of MMP-2 [68], MMP-3 [69], and MMP-13 [70]. Any alteration in these factors would thus have been of interest to observe in a future experiment. Another interesting test would be to test the cells branching capabilities in a 3D branching assay.

In conclusion, the results from this work indicated that S100A4 was not necessary for induction of EMT. Another obvious question is whether mesenchymal cells lacking S100A4 are able revert to an epithelial form through MET. The limiting time frame of this thesis did not allow for any elaboration of this theory, and future perspectives would thus include experimental studies aimed to identify the potential importance of S100A4 for induction of MET.

References

5.1 List of references

1. Foroni, C., Broggini, M., Generali, D., Damia, G., *Epithelial-mesenchymal transition and breast cancer: role, molecular mechanisms and clinical impact.* Cancer Treatment Reviews, 2012. **38**(6): p. 689-97.
2. Boye, K., Maelandsmo, G. M., *S100A4 and metastasis: a small actor playing many roles.* The American Journal of Pathology, 2010. **176**(2): p. 528-35.
3. Strutz, F., Okada, H., Lo, C. W., Danoff, T., Carone, R. L., Tomaszewski, J. E., Nielson, E. G., *Identification and characterization of a fibroblast marker: FSP1.* The Journal of Cell Biology, 1995. **130**(2): p. 393-405.
4. Rudland, P.S., Platt-Higgins, A., Renshaw, C., West, C. R., Winstanley, J. H., Robertson, L., Barraclough, R., *Prognostic significance of the metastasis-inducing protein S100A4 (p9Ka) in human breast cancer.* Cancer Research, 2000. **60**(6): p. 1595-603.
5. Lee, W.Y., Su, W. C., Lin, P. W., Guo, H. R., Chang, T. W., Chen, H. H., *Expression of S100A4 and Met: potential predictors for metastasis and survival in early-stage breast cancer.* Oncology, 2004. **66**(6): p. 429-438.
6. Sternlicht, M.D., *Key stages in mammary gland develompent; The cues that regulate ductal branching morphogenesis.* Breast cancer research, 2006. **8**(1): p. 11.
7. Kåresen, R., Schlichting, E., Wist, E., *Hvordan utvikler det normale kvinne bryst seg fra foster til eldre kvinne?*, in *Brystkreft; En informasjonsbok for pasienter og pårørende*. 1998, Universitets forlaget: Oslo. p. 11-13.
8. Joseph, N. *Breast Mammography: Correlated Ultrasound, MRI, CT, and SPECT-CT*. [Online Radiography Continuing Education for Radiologic X ray Technologist] 2012 2012 [cited 2013 13.04.23]; Available from: http://www.ceessentials.net/article40.html.
9. Fata, J.E., Zena, W., Bissell, M. J., *Regulation of mammary gland branching morphogenesis by the extracellular matrix and its remodeling enzymes.* Breast cancer research, 2004. **6**(1): p. 1-11.
10. WHO. *Cancer*. [Web page] 2012 February 2012 [cited 2012 12.08.13]; Available from: http://www.who.int/mediacentre/factsheets/fs297/en/#.
11. **Naume, B.** *Brystkreft*. 2012 13/01-2012 [cited 2012 13.08.25]; Available from: http://oncolex.no/Bryst.aspx.
12. Bøhler, P.J. *Histologi*. 2012 05.02.2013 [cited 2013 13.05.06]; Available from: http://oncolex.no/Bryst/Bakgrunn/Histologi.aspx.
13. Weigelt, B., Bissell, M. J., *Unraveling the microenvironmental influences on the normal mammary gland and breast cancer.* Seminars in Cancer Biology, 2008. **18**(5): p. 311-321.
14. Damjanov, I., *Pathology for the health professions*, in *Pathology for the health professions*, M. Hutchinson, Editor. 2006, Elsevier Saunders: St. Louis. p. 382, 388-390.
15. Hanahan, D., Weinberg, R. A., *Hallmarks of cancer: the next generation.* Cell, 2011. **144**(5): p. 646-74.
16. Kalluri, R., Weinberg, R. A., *The basics of epithelial-mesenchymal transition.* The Journal of Clinical Investigation, 2009. **119**(6): p. 1420-1428.
17. Alberts, B., Johnson, A., Lewis, J., Raff, M., Roberts, K., Walter, P., *Cancer*, in *Molecular Biology of the Cell*, S.G. Marjorie Anderson, Editor. 2008, Garland Science: New York. p. 1220.
18. Franco, R., Cantile, M., Marino, F. Z., Pirozzi, G., *Circulating tumor cells as emerging tumor biomarkers in lung cancer.* Journal of Thoracic Disease, 2012. **4**(5): p. 438-439.
19. Nguyen, D.X., Bos, P. D., Massagúe, J., *Metastasis: from dissemination to organ-specific colonization.* Nature Reviewes Cancer, 2009. **9**(4): p. 274-284.

20. Sánchez-Tilló, E., Liu, Y., de Barrios, O., Siles, L., Fanlo, L., Cuatrecasas, M., Darling, D. S., Dean, D. C., Castells, A., Postigo, A., *EMT-activating transcription factors in cancer: beyond EMT and tumor invasiveness.* Cellular and molecular life sciences, 2012. **69**(20): p. 3429-3456.
21. Sigma-Aldrich. *Cadherin*. [Web page] 2013 2013 [cited 2013 13.03.01]; Available from: http://www.sigmaaldrich.com/life-science/metabolomics/enzyme-explorer/learning-center/structural-proteins/cadherin.html.
22. Gilles, C., Polette, M., Zahm, J. M., Tournier, J. M., Volders, L., Foidart, J. M., Birembaut, P., *Vimentin contributes to human mammary epithelial cell migration.* Journal of Cell Science, 1999. **112**: p. 4615-4625.
23. Amatangelo, M.D., Goodyear, S., Varma, D., Stearns, M. E., *c-Myc expression and MEK1-induced Erk2 nuclear localization are required for TGFbeta induced epithelial–mesenchymal transition and invasion in prostate cancer.* Carcinogenesis, 2012. **33**(10): p. 1965-1975.
24. Hugo, H., Ackland, M. L., Blick, T., Lawrence, M. G., Clements, J. A., Williams, E. D., Thompson, E. W., *Epithelial--mesenchymal and mesenchymal--epithelial transitions in carcinoma progression.* Journal of Celluar Physiology, 2007. **213**(2): p. 374-383.
25. Radisky, D.C., LaBarge, M. A., *Epithelial-Mesenchymal Transition and the Stem Cell Phenotype.* Cell Stem Cell, 2008. **2**(6): p. 511-512.
26. Morel, A.P., Lievre, M., Thomas, C., Hinkal, G., Ansieau, S., Puisieux, A., *Generation of breast cancer stem cells through epithelial-mesenchymal transition.* PLoS One, 2008. **3**(8): p. e2888.
27. Weinberg, R.A., *14.4 The epithelial-mesenchymal transition is often induced by stromal signals*, in *The Biology of Cancer*, E. Jeffcocl, Editor. 2007, Garland Science: New York, USA. p. 605-614.
28. Alberts, B., Johnson, A., Lewis, J., Raff, M., Roberts, K., Walter, P., *Cell junctions, cell adhesion, and the extracellular matrix*, in *Molecular Biology of the Cell*, S.G. Marjorie Anderson, Editor. 2008, Garland Science: New York. p. 1141.
29. Talbot, L.J., Bhattachvarya, S. D., Kuo, P. C., *Epithelial-mesenchymal transition, the tumor microenvironment, and metastatic behavior of epithelial malignancies.* International Journal of Biochemistry and Molecular Biology, 2012. **3**(2): p. 117-136.
30. Weinberg, R.A., *14.5 EMTs are programmed by transcription factors that orchestrate key steps of embryogenesis*, in *The Biology of Cancer*, E. Jeffcocl, Editor. 2007, Garland Science: New York, USA. p. 615-619.
31. Nelson, W.J., Nusse, R., *Convergence of Wnt, β-Catenin, and Cadherin Pathways.* Science AAAS, 2004. **303**(5): p. 1483-1487.
32. Alberts, B., Johnson, A., Lewis, J., Raff, M., Roberts, K., Walter, P., *Mechanisms of Cell Communication and Cancer*, in *Molecular Biology of the Cell*, S.G. Marjorie Anderson, Editor. 2008, Garland Science: New York. p. 939-941, 1243.
33. Miyazono, K., *Tumour promoting functions of TGF-β in CML-initiating cells.* Journal of Biochemistry, 2012. **152**(5): p. 383-385.
34. Moore, B., *A soluble protein characteristic of the nervous system.* Biochemical and Biophysical Research Communications, 1965. **16**(6): p. 739-744.
35. Garrett, S.C., Varney, K. M., Weber, D. J., Bresnick, E. R., *S100A4, a mediator of metastasis.* The Journal of Biological Chemistry, 2006. **281**(2): p. 677-680.
36. Cunningham, M.F., Docherty, N.G., Burke, J.P., O'Connell, P.R., *S100A4 expression is increased in stricture fibroblasts from patients with fibrostenosing Crohn's disease and promotes intestinal fibroblast migration.* American Journal of Physiology, 2010. **299**(2): p. 457-466.
37. Nubile, N., Lanzini, M., Calienno, R., Mastropasqua, R., Curcio, C., Mastropasqua, A., Agnifili, L., Mastropasqua, L., *S100 A and B expression in normal and inflamed human limbus.* Molecular Vision, 2013. **19**: p. 146-152.
38. Dahlmann, M., Sack, U., Herrmann, P., Lemm, M., Fichtner, I., Schlag, P. M., Stein, U., *Systemic shRNA mediated knock-down of S100A4 in colorectal cancer xenografted mice reduces metastasis formation.* Oncotarget, 2012. **3**(8): p. 783-797.

39. Fujiwara, M., Kashima, T. G., Kunita, A., Komura, D., Grigoriadis, A. E., Kudo, A., Aburatani, H., Fukayama, M., *Stable knockdown of S100A4 suppresses cell migration and metastasis of osteosarcoma.* Tumor Biology, 2011. **32**(3): p. 611-622.
40. Mælandsmo, G.M., Hovig, E., Skrede, M., Engebraaten, O., Florenes, V. A., Myklebost, O., Grigorian, M., Lukanidin, E., Scanlon, K. J., Fodestad, O., *Reversal of the in vivo metastatic phenotype of human tumor cells by an anti-CAPL (mts1) ribozyme.* Cancer Research, 1996. **56**(23): p. 5490-5498.
41. Tabata, T., Tsukamoto, N., Fooladi, A. A. I., Yamanaka, S., Furukawa, T., Ishida, M., Sato, D., Gu, Z., Nagase, H., Egawa, S., Sunamura, M., Horii, A., *RNA interference targeting against S100A4 suppresses cell growth and motility and induces apoptosis in human pancreatic cancer cells.* Biochemical and Biophysical Research Communications, 2009. **390**(3): p. 475-480.
42. Zhang, G., Li, M., Bai, Y., Yang, C., *Knockdown of S100A4 decreases tumorigenesis and metastasis in osteosarcoma cells by repression of matrix metalloproteinase-9.* Asian Pasific Journal of Cancer Research, 2011. **12**(8): p. 2075-2080.
43. Davies, B.R., Davies, M. P., Gibbs, F. E., Barraclough, R., Rudland, P. S., *Induction of the metastatic phenotype by transfection of a benign rat mammary epithelial cell line with the gene for p9Ka, a rat calcium-binding protein, but not with the oncogene EJ-ras-1.* Oncogene, 1993. **8**(4): p. 999-1008.
44. Grigorian, M., Ambartsumian, N., Lykkelsfeldt, A. E., Bastholm, L., Elling, F., Georgiev, G., Lukanidin, E., *Effect of mts1 (S100A4) expression on the progression of human breast cancer cells.* International Journal of Cancer, 1996. **67**(6): p. 831-841.
45. Elenbaas, B., Spirio, L., Koerner, F., Fleming, M. D., Zimonjic, D. B., Donaher, J. L., Popescu, N. C., Hahn, W. C., Weinberg, R. A., *Human breast cancer cells generated by oncogenic transformation of primary mammary epithelial cells.* Genes and Development, 2001. **15**(1): p. 50-65.
46. Gupta, P.B., Onder, T. T., Jiang, G., Tao, K., Kuperwasser, C., Weinberg, R. A., Lander, E. S., *Identification of Selective Inhibitors of Cancer Stem Cells by High-Throughput Screening.* Cell, 2009. **139**(4): p. 645-659.
47. Tveito, S., Andersen, K., Kåresen, R., Fodstad, Ø., *Analysis of EpCAM positive cells isolated from sentinel lymph nodes of breast cancer patients identifies subpopulations of cells with distinct transcription profiles.* Breast cancer research, 2011. **13**(4).
48. EssenBioscience. *Essen Incucyte. You'll never look at cels the same way*. 2012 [cited 2013 13.04.05]; Available from: http://www.sibcb.ac.cn/temp/Incucyte_FLR_2.pdf.
49. PromegaCorporation. *CellTiter 96 AQueous One Solutin Cell Proliferation Assay*. 2004 2004 [cited 2013 13.04.05]; Available from: http://no.promega.com/~/media/files/products%20and%20services/brochures/cell%20analysis/ds233.pdf?la=en.
50. Wang, Z., Rao, D. D., Senzer, N., Nemunaitis, J., *RNA Interference and Cancer Therapy.* Pharmaceutical Research, 2011. **28**(12): p. 2983-2995.
51. Sigma-Aldrich. *MISSION pLKO.1-puro Non-Mammalian shRNA Control Plasmid DNA*. [Web page] 2013 2013 [cited 2013 13.04.02]; Available from: http://www.sigmaaldrich.com/catalog/product/sigma/shc002?lang=en&region=NO.
52. ThermoScientific. *Instructions, Pierce BCA Protein Assay Kit*. 2011 [cited 2013 13.03.21]; 1-7]. Available from: http://www.piercenet.com/instructions/2161296.pdf.
53. LifeTechnologies™. *Novex® Midi Gel System. A system for electrophoresis, blotting, and staining of midi gels*. 2012 February 2012 [cited 2013 13.04.10]; 1-6]. Available from: http://tools.invitrogen.com/content/sfs/manuals/novex_midigel_man.pdf.
54. ThermoScientific. *Chemiluminescent Western blotting technical guide and protocols* 2009 2009 [cited 2013 13.04.10]; Available from: http://www.piercenet.com/files/TR0067-Chemi-Western-guide.pdf.
55. Flatmark, K., Mælansmo, G. M., Mikalsen, S. O., Nustad, K., Veraas, T., Rasmussen, H., Meling, G. I., Fodestad, Ø., Paus, E., *Immunofluorometric assay for the metastasis-related protein S100A4: release of S100A4 from normal blood cells prohibits the use of S100A4 as a tumor marker in plasma and serum.* Tumor Biology, 2004. **25**(1-2): p. 31-40.

56. Invitrogen. *Introduction to Flow Cytometry*. 2012 [cited 2013 13.05.06]; Available from: http://probes.invitrogen.com/resources/education/tutorials/4Intro_Flow/player.html.
57. Semrock. *Filters for Flow Cytometry*. 2013 [cited 2013 13.03.25]; Available from: http://www.semrock.com/flow-cytometry.aspx.
58. QIAGEN. *RNeasy^{R} Mini Handbook*. 2010 September 2010 13.04.10]; 4 th:[39-44]. Available from: http://www.genome.duke.edu/cores/microarray/services/rna-qc/documents/RNeasy_Mini_Handbook.pdf.
59. ThermoScientific. *NanoDrop 2000*. 2009 [cited 2012 12.08.11]; Available from: http://www.nanodrop.com/Productnd2000overview.aspx.
60. Sjøberg, N.O., *14.5 cDNA*, in *Molekylær genetikk, Genteknologi - humant DNA*. 2006, Forlaget vett of viten AS: Nesbru, Norway. p. 182-184.
61. BioRad. *qPCR/Real-Time PCR*. [webpage] 2013 2013 [cited 2013 13.04.07]; Available from: http://www.bio-rad.com/evportal/en/NO/evolutionPortal.portal?_nfpb=true&_pageLabel=SolutionsLandingPage&catID=LUSO4W8UU.
62. Sjøberg, N.O., *14.4 PCR, 18.6 Real-time PCR og DNA smelteprofiler*, in *Molekylær genetikk, Genteknologi - humant DNA*. 2006, Forlaget vett of viten AS: Nesbru, Norway. p. 176-181, 241-243.
63. QuantaBiosciences. *PerfeCTa® qPCR SuperMix*. [webpage] 2013 2013 [cited 2013 13.04.07]; Available from: http://www.quantabio.com/product.php?base_id=95050.
64. Onder, T.T., Gupta, P. B., Mani, S. A., Yang, J., Lander, E. S., Weinberg, R. A., *Loss of E-Cadherin Promotes Metastasis via Multiple Downstream Transcriptional Pathways.* Cancer Res, 2008. **68**(10): p. 3645-3654.
65. Mani, S.A., Guo, W., Liao, M., Eaton, E. N., Ayyanan, A., Zhou, A. Y., Brookes, M., Reinhard, F., Zhang, C. C., Shipitsin, M., Campbell, L. L., Polyak, K., Brisken, C., Yang, J., Weinberg, R. A., *The epithelial-mesenchymal transition generates cells with properties of stem cells.* Cell 2008. **133**(16): p. 704-715.
66. Al-Hajj, M., Clarke, M. F., *Self-renewal and solid tumor stem cells.* Oncogene, 2004. **23**: p. 7274-7282.
67. Chai, J., Jamal, M. M., *S100A4 in esophageal cancer: Is this the one to blame?* World journal of gastroenterology, 2012. **18**(30): p. 3931-3935.
68. Bjørnland, K., Winberg, J. O., Odegaard, O. T., Hovig, E., Loennechen, T., Aasen, A. O., Fodstad, O., Maelandsmo, G. M., *S100A4 involvement in metastasis: deregulation of matrix metalloproteinases and tissue inhibitors of matrix metalloproteinases in osteosarcoma cells transfected with an anti-S100A4 ribozyme.* Cancer Research, 1999. **59**(18): p. 4702-4708.
69. Andersen, K., Mori, H., Fata, J., Bascom, J., Oyjord, T., Maelandsmo, G. M., Bissell, M., *The metastasis-promoting protein S100A4 regulates mammary branching morphogenesis.* Developmental Biology, 2011. **352**(2): p. 181-90.
70. Berge, G., Pettersen, S., Grotterød, I., Bettum, I. J., Boye, K., Mælandsmo, G. M., *Osteopontin--an important downstream effector of S100A4-mediated invasion and metastasis.* International Journal of Cancer, 2011. **129**(4): p. 780-790.

Appendix

6.1 List of Products

Cell culture

Product		Producer	Catalog number
MEGM™ Mammary Epithelial Cell Growth Medium		Lonza	CC-3150
DMEM/F-12, no glutamine.		Gibco® by Life Technologies™	21331-020
Additives to DMEM/F-12	Insulin Solution, Human	Sigma-Aldrich®	I9278
	Hydrocortisone	Sigma-Aldrich®	H0888
	Recombinant human EGF	PeproTech	AF-100-15
	GlutaMAX™ Supplement	Gibco® by Life Technologies™	35050-038
	PEN-STREP	Lonza	DE17-603E
	HEPES Buffer in normal Saline	Lonza	BE17-737E
Trypsin-Versene (EDTA) Mixture (1X)		Lonza	BE 17-161E
Nunclon™ surface 6 well plate		Thermo scientific	140675
Nunclon™ surface 24 well plate		Thermo scientific	142475
Nunclon Delta Surface, 96 well Plate		Thermo Scientific	167008
Clear 96-well Microtest™ Plate		BD Falcon™	3072
Nunclon™ surface, 25 ml		Thermo scientific	156367
Nunclon™ surface, 75 ml		Thermo scientific	156499
Glasstic slide 10 with counting grids		KOVA®	87144 E
Dynabeads Sheep anti-Mouse IgG		Life Technologies™	110.31
Dimethyl sulfoxide (DMSO)		Sigma-Aldrich	D2650
Fetal calf serum (FCS)		Paa Laboratories GmbH	A15-101
32 % Paraformaldehyd		Chemi-Teknik as/Electron Microscopy Sciences	15714

Recombinant Human TGF-β1	R&D systems®	240-B-002
Trypan Blue Stain, 0.4 %	GIBCO®	15250-061
Countess™ Cell Counting Chamber Slides	Invitrogen™	C10283
CellTiter 96® AQ_{ueous} One Solution Reagent	Promega	G3580
PBS without Ca^{2+}, Mg^{2+} and phenol red	Lonza	BE 17-516F
CryoTube® Vials	Thermo Scientific	363401
Sterile Water	B. Braun	7534
Venor®GeM Mycoplasma PCR Detection Kit	Minerva Biolabs®	11-1100
Antibac Overflatedesinfeksjon	Antibac® AS	600521

Immunofluorescence microscopy

Product	**Producer**	**Catalog number**
NH_4Cl. Ammonium chloride	KEBOLabs	Unknown
SuperFrost® Plus	Thermo Scientific	J1800AMNZ
Anti E-cadherin antibody (DECMA-1)c (FAM)	abcam®	ab11512
Alexa Fluor® 568 Goat Anti-Rat IgG (H+L)	Invitrogen	A11077
Saponin from quialla bark	Sigma-Aldrich	S7900-25G
ProLong® Gold Antifade Reagent with DAPI	Life Technologies™	P36935
Glycine	VWR	1.04201.1000

Lentiviral transduction

Product	**Producer**	**Catalog number**
Antibac Overflatedesinfeksjon	Antibac® AS	600521
Klorin	Lilleborg	Unknown
MISSION® pLKO. 1-Puro Non-Mammalian shRNA Control Transduction Particles	Sigma-Aldrich	SHC002V
MISSION® shRNA Lentiviral Transduction Particles	Sigma-Aldrich	SHCLNV-NM_002961, TRCN0000053610
Hexadimethrine bromide	Sigma-Aldrich	H9268
Puromycin	Sigma-Aldrich	P9620
Rely+On™ Virkon®	DuPont™	Unknown

Western blot

Product	Producer	Catalog number
Sodium chloride	Merck	1.06404.1000
Triton® x-100	VWR	28817.295
Sodium deoxycholate	Sigma-Aldrich	D6750
SDS (soudium dodecyl sulphate)	Merck	822050
UltraPure™ Tris 1M	Gibco by Life Technologies	15567-027
Tween® 20	Merck	655204
Complete, mini protease inhibitor cocktail tablets	Roche	04693124001
phosSTOP	Roche	04906837001
Bovine Serum Albumin Standard Ampules, 2 mg/ml	Thermo Scientific	23209
BCA Protein Assay Reagent A	Thermo Scientific	23228
BCA Protein Assay Reagent B	Thermo Scientific	1859078
Nunclon Sterile 96 Well Plate with lid	Thermo Scientific	167008
NuPAGE® Sample Reducing Agent (10x)	Invitrogen	NP0009
NuPAGE® LDA Sample Buffer (4x)	Invitrogen	NP0008
NuPAGE® Novex 4-12 % Bis-Tris Gel 1,5 mm, 10 well	Invitrogen	NP0335BOX
NuPAGE® Novex 4-12 % Bis-Tris Midi Gel, 12+2 well	Invitrogen	WG1401BOX
NuPAGE® Novex 4-12 % Bis-Tris Midi Gel, 20 well	Invitrogen	WG1402BOX
NuPAGE® MES SDS Running Buffer (for Bis-Tris Gels only) (20X)	Invitrogen	NP0002
SeeBlue® Plus2 Pre-Stained Standard	Invitrogen	LC5925
iBlot® Transfer Stack, Regular (Nitrocellulose)	Invitrogen	IB3010-01
Monoclonal anti-S100A4, clone 22.3	*Flatmark et al., 2004* [55]	In-house
Anti-α-Tubulin Mouse (DM1A) Antibody	Millipore	CP06-100UG
Polyclonal Rabbit Anti-Mouse Immunoglobulins/HRP	DAKO	P0260
SuperSignal® West Dura Extended Duration Substrate	Thermo Scientific	34076

Flow cytometry

Product	Producer	Catalog number
γ-Globulins from human blood (Flow cytometry buffer)	Sigma-Aldrich	G-4386
Round-Bottom Tube	BD Falcon™	352054
Round-Bottom Tube	BD Flacon™	352235
PBS without Ca^{2+}, Mg^{2+} and phenol red	Lonza	BE 17-516F
BD FACS Flow Sheath Fluid	BD FACSFlow™	342003
BD FACS Clean solution	BD FACS™	340345
BD FACS Rinse solution	BD FACS™	340346
Hoechst 33258	Sigma-Aldrich	861405
PerCP-Cy™ 5.5 anti-EpCAM Clone EBA-1	BD Biosciences	347199
APC anti-human CD326 (EpCAM) Clone 9C4	BioLegend®	324208
APC Mouse Anti-Human CD44 Clone G44-26	BD Biosciences	559942
FITC Mouse Anti-Human CD24 ML5	BD Biosciences	555427
PE Mouse Anti-Human CD24 Clone ML5	BD Biosciences	560991
FITC Mouse Anti-Human CD44 Clone G44-26	BD Biosciences	555478
PE anti-human CD326 (EpCAM) Antibody Clone 9C4	BioLegend®	324205

Reverse transcription qPCR

Product	Producer	Catalog number
QIAshredder™	QIAGEN	79654
RNeasy® Mini Kit	QIAGEN	74104
β-mercaptoethanol	Sigma-Aldrich	M-6250
qScrpit™ cDNA Synthesis Kit	Quanta BioSciences	95047-100
0.2 mL PCR Tubes	Thermo Scientific	AB-0620
PerfeCTa® qPCR SuperMix	Quanta BioSciences	95050-500
iQ™ 96-Well PCR Plate	Bio-Rad	223-9441
Absolutt alkohol	Kemetyl Norge AS	200-578-6

Appendix

YARS	Eurogentec	Forward: 4721522
		Reverse: 4721523
TBP	Eurogentec	F: 743466
		R: 743467
S100A4	Eurogentec	F: 4370419
		R: 4370420
CDH1	Eurogentec	F: 4370413
		R: 4370414
CDH2	Eurogentec	F: 4069108
		R: 4069109
VIMENTIN	Eurogentec	F: 2133606
		R: 2133607
SNAI1	Eurogentec	F: 4370417
		R: 4370418
SNAI2	Eurogentec	F: 4058443
		R: 4058444
ZEB1	Integrated DNA Technologies®	F: 64538163
		R: 64538162
ZEB2	Integrated DNA Technologies®	F: 64538165
		R: 64538164
Probe #3	Roche - Universal ProbeLibrary	04 685 008 001
Probe #7	Roche - Universal ProbeLibrary	04 685 059 001
Probe #16	Roche - Universal ProbeLibrary	04 686 896 001
Probe #20	Roche - Universal ProbeLibrary	04 686 934 001
Probe #35	Roche - Universal ProbeLibrary	04 687 680 001
Probe #47	Roche - Universal ProbeLibrary	04 688 074 001
Probe #62	Roche - Universal ProbeLibrary	04 688 619 001
Probe #66	Roche - Universal ProbeLibrary	04 688 651 001

Probe #81	Roche - Universal ProbeLibrary	04 689 046 001

6.2 List of Instruments and Software

Instrument	**Producer**	**Software**
Cell culture		
Biowizard Gloden Line	Kojair®	--
Thermo Scientific Forma Steri-Cycle CO_2 Incubators	Thermo Scientific	--
Centrifuge 5810	Eppendorf	--
Countess® automated cell counter	Invitrogen	Countess®
Leica DM IL	Leica	--
IX81	Olympus	Cell^P
X-Cite® 120PC Q	Lumen Dynamics	Cell^P
Incucyte FLR	Essen Bioscience	IncuCyte 2011A
Modulus™ Microplate	Turner BioBystems	GloMax® Multi Detection system
Western		
Ultrasonic Homogenizer 4710 series	Cole Parmer	--
QBT2 Heating Block	Grant	--
PowerEase500	Inivtrogen	--
XCell4 Surelock™ Midi-Cell	Inivtrogen	--
iBlot™	Invitrogen	--
G:BOX	Syngene	GeneSnap
Flow Cytometry		
BD LSR II Flow Cytometer	BD Biosciences	BD FACSDiva software FlowJo_V10.0.5
RT-qPCR		
NanoDrop 2000 Spectrophotometer	Thermo Scientific	NanoDrop 2000/2000c
GeneAmp® PCR System 9700	Applied Biosystems	--
iCycler™	Bio-Rad	iCycler Genex

6.3 Solutions

Supplements to the DMEM/F12 growth media:

10 ng/ml	rhEGF (PeproTech)
0,5 µg/ml	Hydrocortisone (Sigma-Aldrich)
10 µg/ml	Insulin (Sigma-Aldrich)
50 IU/ml (Pen)	Pen/Strep (Lonza)
50 IU/ml (Strep)	
20 mM	HEPES (Lonza)
2 mM	Glutamax (Gibco by Life Technologies)

RIPA buffer:

150 mM	Sodium chloride
1.0 %	NP-40 or Triton X-100
0.5 %	Sodium deoxycholate
0.1 %	SDS (sodium dodecyl sulphate)
50 mM	Tris, pH 8.0

Add 1 Complete, mini protease inhibitor cocktail tablet to 2 ml ddH_2O (5x)
Add 1 phosSTOP (phosphatase inhibitor) tablet to 2 ml ddH_20 (5x)

50 µl protease inhibitor and 50 µl phosphatase inhibitor was added to 1 ml lysis buffer.

Research and development buffer (R&D-buffer):

0,1 %	20 % Tween
0,15 M	5 M NaCl
25 mM	1 M Tris